Am J Cancer Res 2022;12(6):2465-2491
www.ajcr.us /ISSN:2156-6976/ajcr0141528

Original Article

Long non-coding RNA lncHUPC1 induced by FOXA1 promotes tumor progression by inhibiting apoptosis via miR-133b/SDCCAG3 in prostate cancer

Miao Liu[1,2*], Ai Shen[3*], Yongbo Zheng[1], Xiong Chen[1], Leilei Wang[4], Ting Li[4], Xin Ouyang[1], Xian Yu[2], Hao Sun[2], Xiaohou Wu[1]

[1]Department of Urology, The First Affiliated Hospital of Chongqing Medical University, Chongqing, China; [2]Gastrointestinal Cancer Center, Chongqing University Cancer Hospital, Chongqing, China; [3]Hepatobiliary and Pancreatic Tumor Center, Affiliated Cancer Hospital of Chongqing University, Chongqing, China; [4]Key Laboratory of Laboratory Medical Diagnostics, Ministry of Education, Chongqing Medical University, Chongqing, China. [*]Co-first authors.

Received January 4, 2022; Accepted May 9, 2022; Epub June 15, 2022; Published June 30, 2022

Abstract: Long non-coding RNAs (lncRNAs) were confirmed to be involved in regulating various malignant behaviors of tumor cells in prostate cancer (PCa). Using The Cancer Genome Atlas (TCGA) prostate adenocarcinoma datasets, several endogenous competing RNA (ceRNA) networks of lncRNA/miRNA/mRNA associated with the progression-free survival (PFS) and Gleason score (GS) were identified using bioinformatics analysis. lncRNA AC004447.2 (lncHUPC1, ENSG00000269131)/miR-133b/serologically defined colon cancer antigen-3 (SDCCAG3) was a newly identified ceRNA network that affected cell growth and apoptosis in PCa. Using q-PCR, lncHUPC1 and SDCCAG3 were found to be up-regulated in PCa cells, while miR-133b was down-regulated. The same results were found in tissue samples from 70 PCa cases. It was confirmed that the knockdown of lncHUPC1 increased the expression of miR-133b and decreased that of SDCCAG3, which further increased apoptosis and inhibited cell growth, while the miR-133b inhibitor partially reversed these effects. After transfection with miR-133b mimic after lncHUPC1-knockdown, the expression of miR-133b increased while that of SDCCAG3 reduced, and the apoptosis of the cells was more obvious and the growth of the cells was slower. Therefore, lncHUPC1 was confirmed to regulate SDCCAG3 by binding to miR-133b. Additionally, we found that the transcription factor Forkhead Box A1 (FOXA1) directly bound to the promoter of lncHUPC1 to activate it. In conclusion, the ceRNA network of lncHUPC1/miR-133b/SDCCAG3 affected the growth and apoptosis of PCa cells, and FOXA1 may be involved in the process as a transcription factor of lncHUPC1.

Keywords: Prostate cancer, lncRNAHUPC1, miR-133b, SDCCAG3, FOXA1

Introduction

According to the "Global Cancer Statistics 2018" released by the World Health Organization, PCa is the second most common cancer in men. In 2018, there were a total of 1.276 million new cases of PCa worldwide [1]. Also, in Asian countries, the rate is increasing substantially. The etiology and pathogenesis of PCa are still unclear [2]. The main treatment of PCa is surgical resection, and the treatment efficacy in advanced PCa is not good. Exploring the etiology and pathogenesis of PCa has important clinical significance for the early diagnosis of the disease and the identification and development of targeted drugs [3].

Long-chain non-coding RNA (lncRNA) is an important non-coding RNA. Its length exceeds 200 nucleotides and it performs a wide range of functions [4]. miRNA is an endogenous non-coding RNA consisting of 20-25 nucleotides. In the cytoplasm, miRNA can bind to the 3'-non-coding region of the target gene mRNA, leading to the degradation of the mRNA or inhibition of its translation, and downregulation of the expression of the target gene. Some lncRNA can be seen as a natural "molecular sponge" in the cytoplasm, which can absorb a large amount of miRNA by interfering with the 3'-untranslated regions (3'-UTR) of miRNA and inhibit the effect of miRNA on target genes, and therefore, reduce the ability of miRNAs to inter-

fere with their target genes. The lncRNA, miRNA, and mRNA form a ceRNA [5]. For instance, Wu et al. found that after PAX5 induced the activation of lncRNA forkhead box P4 antisense RNA 1 (FOXP4-AS1), it up-regulated FOXP4 by adsorbing miR-3184-5p and promoted growth of PCa cells [6]. Zhang et al. found that PCA3 up-regulated the expression of high mobility group protein 1 (HMGB1) by binding to miR-218-5p and promoted the progression of Pca [7]. SDCCAG3 interacted with Protein tyrosine phosphatase non-receptor type 13 (PTPN13) via the FERM domain to regulate cytokinesis in colon cancers, which controlled the termination of Fas signal, inhibiting apoptosis in tumor cells [8, 9]. As an important factor in gene transcription and post-transcriptional regulation, transcription factors (TFs) also participate in the regulation of lncRNA-related signaling pathways. For example, the transcription factors FOXA1 and cAMP-response element binding protein 1 (CREB1) were related to advanced PCa, and CREB1/FOXA1 target genes could predict the recurrence of Pca [10]. However, the mechanisms underlying the regulation by miRNA, lncRNA, TFs, and mRNA in PCa need further elucidation.

TCGA database of the Cancer Genome Atlas is a cancer research project jointly conducted by the National Cancer Institute (NCI) and the National Human Genome Research Institute (NHGRI). In the current work, the role of lncRNA AC004447.2 (ENSG000000269131), a cancer promoting lncRNA, in PCa was analyzed using the TCGA database. No relevant public literature on other tumor cells was available. According to the naming principle of HGNC (Hugo Gene Nomenclature Committee) [11], lncRNA AC004447.2 (ENSG000000269131) was named lncHUPC1 (highly up-regulated 1 in prostate cancer). The current study used databases, clinical samples, and data from in vivo and in vitro experiments to elucidate a pathway that inhibited PCa cell apoptosis and promoted PCa growth, which helped understand the molecular mechanism underlying the occurrence and development of PCa and provided valuable clues for further research.

Materials and methods

Database analysis and primary analysis

The Prostate Adenocarcinoma (PRAD) dataset was selected from TCGA [12]. Data on 440 patients whose histological type was Prostate Adenocarcinoma Acinar Type were included in the analysis (440 PCa tissue, 48 normal prostate tissue). Because there were few overall survival events of patients in this dataset, progression-free survival (PFS) was selected as the prognostic parameter for analysis. The "limma" package of R software was used to perform differential analysis. Genes between tumor and normal prostate tissues with fold change (FC) > 1.5 or FC < 2/3 equivalent to $|\log_2 FC| > 0.584963$ and adjust *p*-value < 0.01 were considered as significantly differentially expressed genes. The Cox regression was used for survival analysis and $P < 0.01$ were considered as a significant difference. The online databases LncBase [13], miRWalk [14], and Targetscan [15] were used to predict the targets of lncRNA, miRNA, and mRNA, respectively.

Tissue samples

The tissue samples used in the current study were obtained from 70 PCa patients at the First Affiliated Hospital of the Chongqing Medical University (Chongqing, China) between November 2018 and November 2021. After the samples were obtained, they were frozen using liquid nitrogen and stored at -80°C. **Table 1** shows the clinical characteristics of patients with PCa.

Cell lines and cell culture

The human normal prostate cell line (RWPE-1) and 4 different PCa cell lines (LNCaP, 22RV1, DU145, and PC3) were purchased from the Cell Bank of the Chinese Academy of Sciences (Shanghai, China). All PCa cell lines were cultured in the Roswell Park Memorial Institute (RPMI) 1640 medium (Gibco, Grand Island, NY, USA) with 10% fetal bovine serum (FBS) (Gibco, Grand Island, NY, USA) and 1% Penicillin-Streptomycin (Gibco, USA). RWPE-1 cells were cultured in a special prostate epithelial cell culture medium (PEpiCM, ScienCell, USA) containing prostate epithelial cell growth supplement (PEpiCGS, USA), 10% fetal bovine serum, 1% cereal Aminoamide. All cell lines were cultured in a humidified incubator containing 5% CO_2 at a constant temperature of 37°C.

Cell transfection

sh negative control (sh control) and sh-lncHUPC1 lentiviruses were purchased from Han

Table 1. The clinical characteristics associated with lncHUPC1 expression in PCa

Characters	N = 70	lncHUPC1 levels		*p*-value
		High (n = 35)	Low (n = 35)	
Age (Years)				0.4731
≥ 70	36	20	16	
< 70	34	15	19	
PSA (ng/ml)				0.0109*
< 10	23	6	17	
≥ 10	47	29	18	
Gleason score				0.0079**
≤ 7	40	14	26	
> 7	30	21	9	
Vascular invasion				0.4274
Yes	20	12	8	
No	50	23	27	
Extracapsular metastasis				0.5602
Yes	15	6	9	
No	55	29	26	
Lymph node metastasis				0.4751
Yes	9	6	3	
No	61	29	32	
TNM				0.0083**
I-II	32	10	22	
III-IV	38	25	13	
Endocrine therapy				0.6694
Yes	6	4	2	
No	64	31	33	

*P < 0.05, **P < 0.01.

Heng Biotechnology (Shanghai, China). The microRNA-133b mimic (miR-133b mimic), microRNA-133b inhibitor (miR-133b inhibitor), microRNA negative control (miR NC), FOXA1 siRNA (si-FOXA1), SDCCAG3 siRNA (si-SDCCAG3), and siRNA negative control (si-NC) were purchased from RiboBio Co., Ltd. (Guangzhou, China). Cell transfection was performed according to the instructions provided by the respective manufacturer.

Quantitative real-time polymerase chain reaction (q-PCR)

According to the manufacturer's protocol, TRIzol (Invitrogen) was used to extract total RNA from PCa tissues and cells. All lncRNA, miRNA, and mRNA in this experiment were reverse-transcribed into cDNA using PrimeScript™ RT Master Mix purchased from Takara Biomedical Technology Co. (Beijing, China). Platinum SYBR-Green q-PCR SuperMix (Invitrogen) was used for q-PCR. The normalization control used for miRNA was U6, and that for lncRNA and mRNA was Actin. The primers used in the study were manufactured by Qingdao Biotechnology Co., Ltd. (Beijing, China). The q-PCR primer sequences were as follows: lncHUPC1: 5'-ATAAACCCAAACTCCATCCTCC-3,5-CTTTCTTTAAGCCACAGACTTCCTA-3'. miR-133b: 5'-CTCAACTGGTTCGTGGAGTCGGCAATTCAGTTGAGTAGCTGGT-3,5-ACACTCCAGCTGGGTTTGGTCCCCTTCAAC-3'. SDCCAG3: 5'-GACGCTTGAGCGGAAGTTAGA-3,3-GCCTTTACAGCCCGTTTGG-5'. FOXA1: 5'-GAAGATGGAAGGGCAT-3,5-GCCTGAGTTCATGTTGCTGA-3'. U6: 5'-CTCGCTTCGGCAGCACA-3,5-AACGCTTCACGAATTTGCGT-3'. Actin: 5'-CACCCAGCACAATGAAGATCAAGAT-3,5-CCAGTTTTTAAATCCTGAGTCAAGC-3'.

Cell counting kit-8 (CCK-8)

The trypsinized cell suspension was diluted with culture medium to 4 × 10^4 cells/ml and inoculated in a 96-well plate. After 24 hours of

inoculation, CCK-8 reagent (Hanbio Technology) was added and the cells were incubated in a humidified incubator for 2 hours. Absorbance was measured at 450 nm using a microplate reader. These detection steps were repeated on days 1, 2, 3, and 4 after vaccination.

Colony formation assay

The cells in the logarithmic growth phase were seeded on a 6-well plate (1×10^3/well) after resuspension and counting. After culturing the cells for 10-14 days, the colonies were visible to the naked eye. The cell colonies were fixed with methanol for 20 minutes, then stained with 0.5% crystal violet for 20 minutes, and then imaged.

Cell apoptosis analysis

Hoechst 33342/PI Double Stand Kit (Solarbio, Beijing, China) was used to measure the rate of apoptosis according to the manufacturer's protocol. The treated samples were then subjected to flow cytometry analysis and fluorescence microscopy for observation.

Western blotting

The lysate and Phenylmethanesulfonyl fluoride (PMSF) were used to extract total protein from the cells, and the concentration of total protein was determined using the Bicinchonininc acid (BCA) method. An appropriate amount of protein was taken for sodium dodecyl sulfate-polyacrylamide gel electrophoresis (SDS-PAGE). After electrophoresis, the protein was transferred to polyvinylidene fluoride (PVDF) membranes. These PVDF membranes were blocked with TBS + Tween (TBST) prepared with 5% skimmed milk, at room temperature for 1 hour. Then, the primary antibodies were added and the membranes were incubated overnight at 4°C. Then, the corresponding secondary antibodies were added and the membranes were incubated at room temperature for 1 hour. ECL western blot substrate (Thermo Fisher Scientific) was added to the film for exposure and imaging. SDCCAG3, FOXA1, cleaved Cas8, cleaved Cas3 and β-actin primary antibodies and the corresponding secondary antibodies were purchased from Abcam (UK).

In situ hybridization of the lncRNA fish probe

lncRNA fish probe *in situ* hybridization assay was performed to detect lncHUPC1 cell localization. FISH Probe Mix targeting 18S rRNA, U6, and lncHUPC1 were designed and synthesized by Guangzhou RiboBio Biotechnology Co., LTD. RiboBio's RiboTM Fluorescent In Situ Hybridization Kit was used and hybridization was performed according to the manufacturer's protocol.

Immunohistochemistry (IHC)

The paraffin-embedded tissue sections were stained with HE to determine whether the tissue was cancerous or non-cancerous. The PCa tissues were assigned Gleason scores according to the rules. The sections were stained with Ki67, SDCCAG3, and cleaved Cas8 immunohistochemical stains to assess the corresponding protein levels. Finally, the K-viewer scanning microscope imaging system was used to view the slides. Ki67 results were evaluated using the percentages of positive cells, and other indicators (SDCCAG3, cleaved Cas8 and FOXA1) were evaluated using the immunohistochemistry scores. The staining intensity used to score was - 0 for no stain, 1 for weak stain, 2 for medium stain, and 3 for strong stain. Finally, the percentage of positive cells × staining intensity score was used to calculate the final score.

Luciferase reporter assays

The wild-type (wt) and mutant (mut) sequences of lncHUPC1 and the mutated (mut) and the 3'UTR sequences of SDCCAG3 were designed and cloned into the PHY-811 vector (Guangzhou RiboBio Co., Ltd., China). The wt or mut luciferase plasmid and miRNA mimic were co-transfected into the 22RV1 cells in the same culture dish. The lncHUPC1 promoter was cloned and inserted into the pGL3 basic vector (GeneCreate Biological Engineering Co., Ltd., Wuhan, China), and the pGL3-lncHUPC1 vector was co-transfected with si-control or si-FOXA1. Then, the luciferase activity was detected using the dual-luciferase reporter gene detection system using the manufacturer's (Promega, USA) instructions, 48 hours after transfection.

Chromatin immunoprecipitation (ChIP)

The ChIP kit (Beisinbo, Guangzhou, China) was used to study the intracellular interaction between FOXA1 and lncHUPC1 promoters, according to the manufacturer's protocol. Cells

were cross-linked with 1% formaldehyde, quenched in glycine solution, and treated with ultrasonic shattering to an average length of 200-1000 bp. Then, immunoprecipitation was performed using FOXA1 antibody (Abcam, UK) and IgG control.

Chromatin isolation by RNA purification assays

Six oligonucleotide probes corresponding to the lncHUPC1 transcript were synthesized by RiboBio Co., Ltd. (Guangzhou, China), and the biotin label was located at the 3' end. The probes were divided into two pools (even and odd probe groups) to eliminate non-specific signals. The probe with LacZ as the target was set as a negative control. Chromatin was separated by RNA purification (ChIRP) analysis using the ChIRP kit (Beisinbo, Guangzhou, China) according to the manufacturer's protocol. The enrichment of lncHUPC1 by miR-133b was identified and quantitatively analyzed using q-PCR.

Rapid-amplification of cDNA ends

TRIzol Plus RNA Purification Kit (Invitrogen) was used to extract total RNA from the 22RV1 cells. lncHUPC1 cDNA was used as a template to design primer sequences, and Primer Premier 6.0 software was used to design the 5'/3'RACE primers. Two rounds of nested PCR were performed. The PCR product showed a specific band after electrophoresis. After the gel was cut and the bands were recovered, the pGM-T vector was used to transform the high-efficiency chemically competent DH5α cells, and then, the sequencing analysis was performed.

Animal models

The subcutaneous tumor transplantation model and bone metastasis model were established using nude mice to evaluate the growth and metastasis of PCa cells *in vivo*. A total of 16 4-week-old male nude mice were purchased from SLAC Experimental Animal Center, Chinese Academy of Sciences, Shanghai, and randomly divided into 4 groups (4 mice in each group). 22RV1 cells transfected with lentivirus-packed lncHUPC1 knockdown system (sh lncHUPC1 group) and empty lentivirus (sh control group) were used. In the xenogenous subcutaneous tumor transplantation model, 22RV1 cells from the two transfected groups were subcutaneously injected into the left back of the mice at a rate of 1×10^6 cells/needle. Tumor size was measured every 7 days. Tumor volume was calculated using the formula: tumor volume = 0.52 × (long diameter) × (short diameter)^2. After 4 weeks, the subcutaneous tumor was removed and weighed. The transfected 22RV1 cells from the above two groups (1×10^6 cells/needle) were injected into the tibial nodule of nude mice to establish the bone metastases model (also 4 mice in each group). The mice were sacrificed 6 weeks later and bone metastases were examined using X-ray images. Subcutaneous tumor and bone metastasis were dissected and the ratio of the weight of bone metastasis to the weight of a single hind leg of nude mice was calculated. Pathological sections of both subcutaneous and bone metastases were prepared and stained with HE and IHC. The animal experiments were approved by the Animal Protection and Utilization Committee of the Chongqing Medical University.

Statistical analysis

The data are presented as mean ± standard deviation, and each experiment was replicated at least 3 times independently. GraphPad Prism V5.0 (San Diego, CA, USA) and SPSS software 24.0 (SPSS Inc., Chicago, IL, USA) were used to perform student t-test and ANOVA. Kaplan-Meier method, logarithmic rank test, and Pearson correlation analysis were performed to assess statistical significance. The $P < 0.05$ was considered statistically significant.

Results

Database analysis showed that lncHUPC1, miR-133b and SDCCAG3 had differences in expression and PFS in PCa

A total of 208 lncRNAs were identified to be up-regulated and 71 lncRNAs were down-regulated (**Figure 1A**). 1079 lncRNAs were negatively correlated with PFS, and 95 lncRNAs were positively correlated with PFS. On the whole, 44 up-regulated lncRNAs negatively related to PFS ($HR > 1$, $P < 0.01$) and 11 down-regulated lncRNAs positively related to PFS were identified ($HR < 1$, $P < 0.01$) (**Figure 1B**).

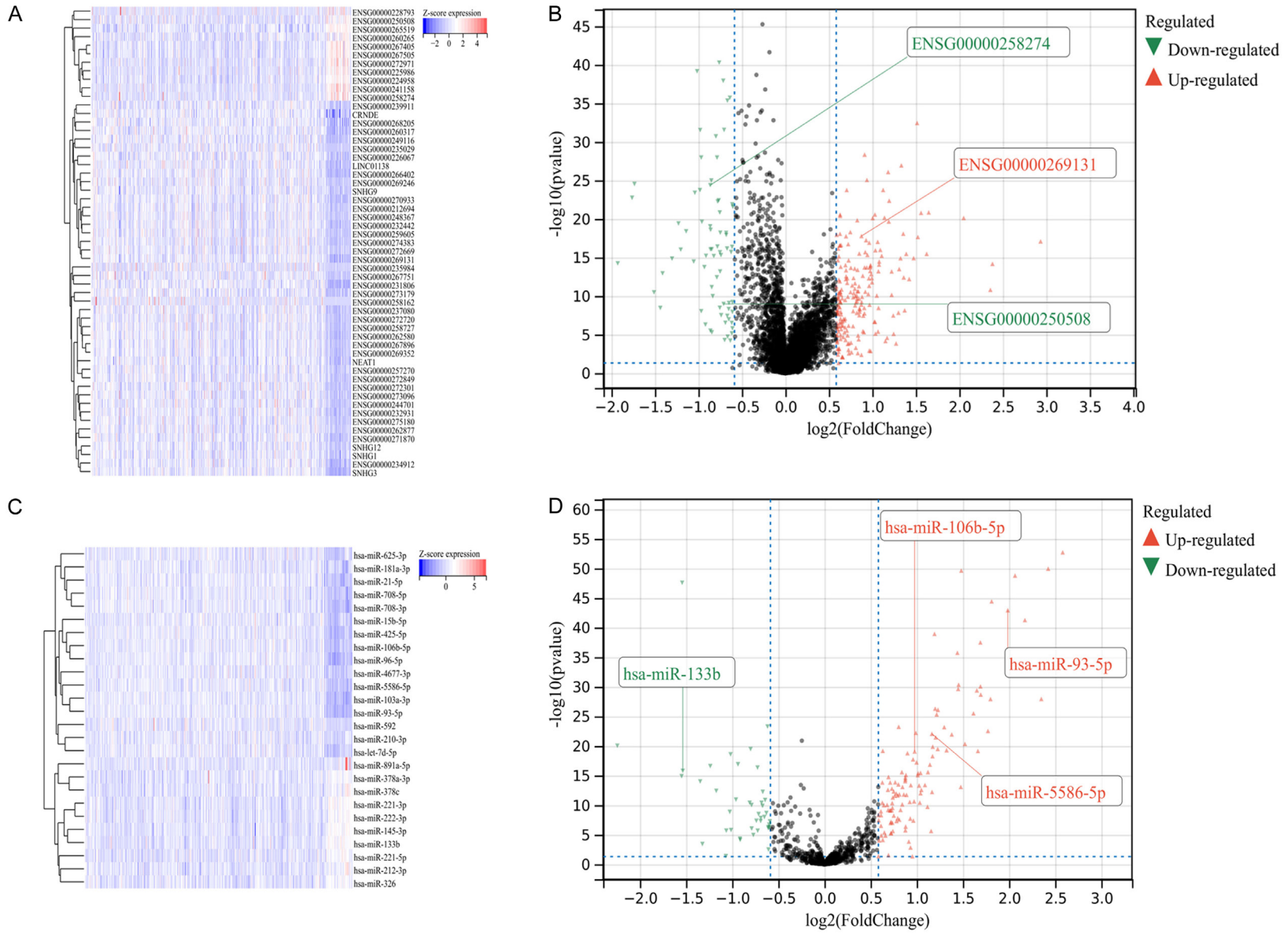
A
Z-score expression
−2 0 2 4
ENSG00000228793
ENSG00000250508
ENSG00000265519
ENSG00000260265
ENSG00000267405
ENSG00000267505
ENSG00000272971
ENSG00000225986
ENSG00000224958
ENSG00000241158
ENSG00000258274
ENSG00000239911
CRNDE
ENSG00000268205
ENSG00000260317
ENSG00000249116
ENSG00000235029
ENSG00000226067
LINC01138
ENSG00000266402
ENSG00000269246
SNHG9
ENSG00000270933
ENSG00000212694
ENSG00000248367
ENSG00000232442
ENSG00000259605
ENSG00000274383
ENSG00000272669
ENSG00000269131
ENSG00000235984
ENSG00000267751
ENSG00000231806
ENSG00000273179
ENSG00000258162
ENSG00000237080
ENSG00000272720
ENSG00000258727
ENSG00000262580
ENSG00000267896
ENSG00000269352
NEAT1
ENSG00000257270
ENSG00000272849
ENSG00000272301
ENSG00000273096
ENSG00000244701
ENSG00000232931
ENSG00000275180
ENSG00000262877
ENSG00000271870
SNHG12
SNHG1
ENSG00000234912
SNHG3
B
Regulated
Down-regulated
Up-regulated
ENSG00000258274
ENSG00000269131
ENSG00000250508
-log10(pvalue)
log2(FoldChange)
C
Z-score expression
0 5
hsa-miR-625-3p
hsa-miR-181a-3p
hsa-miR-21-5p
hsa-miR-708-5p
hsa-miR-708-3p
hsa-miR-15b-5p
hsa-miR-425-5p
hsa-miR-106b-5p
hsa-miR-96-5p
hsa-miR-4677-3p
hsa-miR-5586-5p
hsa-miR-103a-3p
hsa-miR-93-5p
hsa-miR-592
hsa-miR-210-3p
hsa-let-7d-5p
hsa-miR-891a-5p
hsa-miR-378a-3p
hsa-miR-378c
hsa-miR-221-3p
hsa-miR-222-3p
hsa-miR-145-3p
hsa-miR-133b
hsa-miR-221-5p
hsa-miR-212-3p
hsa-miR-326
D
Regulated
Up-regulated
Down-regulated
hsa-miR-106b-5p
hsa-miR-93-5p
hsa-miR-133b
hsa-miR-5586-5p
-log10(pvalue)
log2(FoldChange)

E

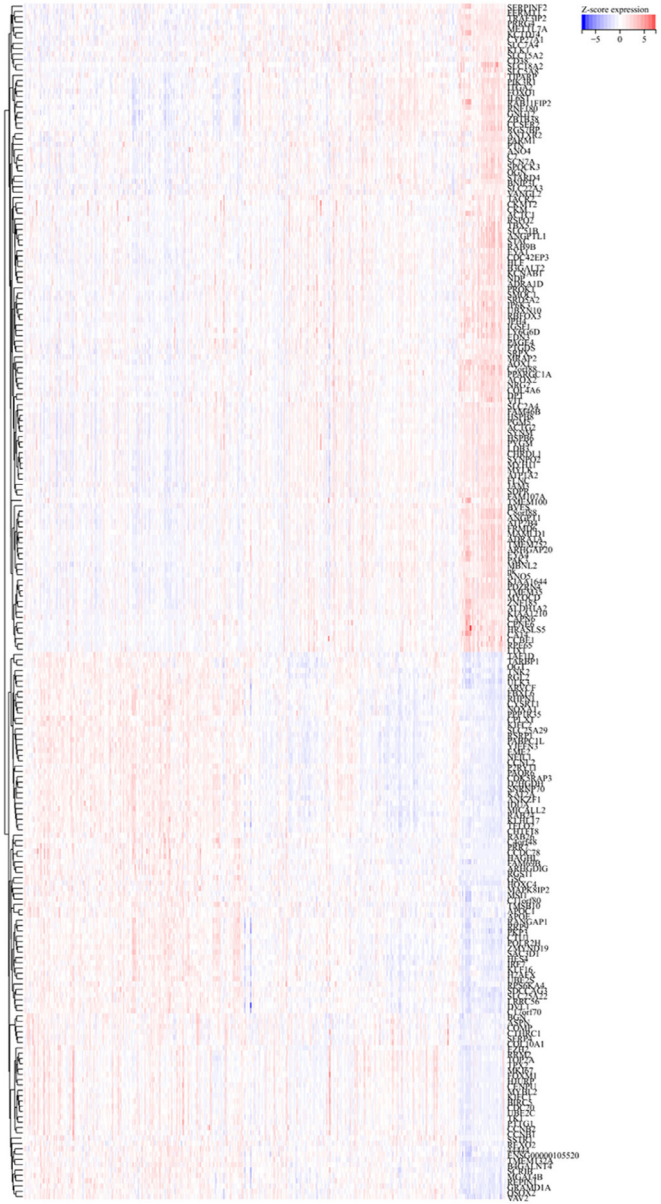
Z-score expression
−5
0
5

F

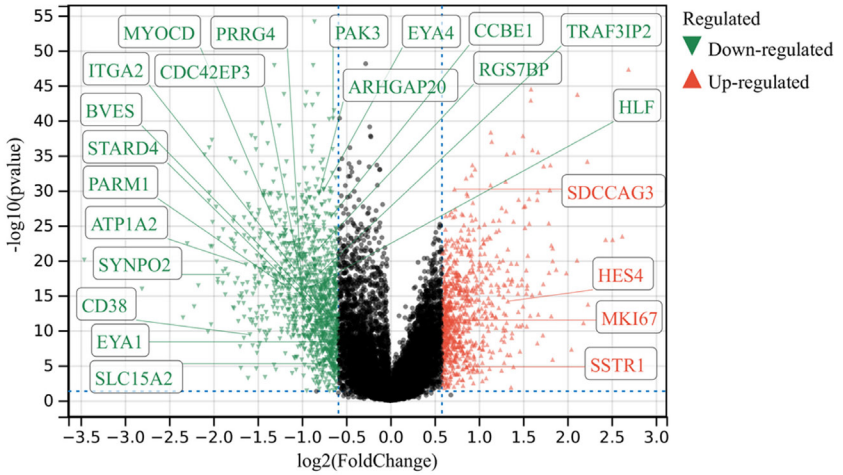
MYOCD
PRRG4
PAK3
EYA4
CCBE1
TRAF3IP2
ITGA2
CDC42EP3
ARHGAP20
RGS7BP
BVES
HLF
STARD4
PARM1
SDCCAG3
ATP1A2
SYNPO2
HES4
CD38
MKI67
EYA1
SSTR1
SLC15A2
-log10(pvalue)
log2(FoldChange)
Regulated
Down-regulated
Up-regulated

G

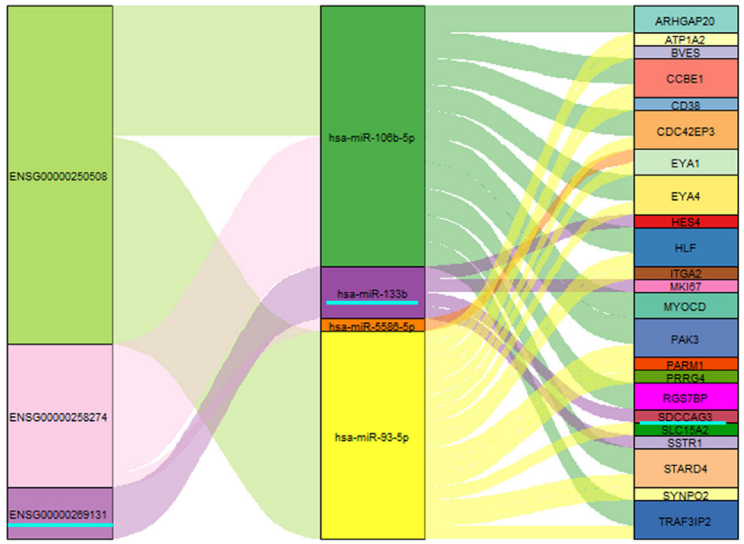
ENSG00000250508
ENSG00000258274
ENSG00000269131
hsa-miR-106b-5p
hsa-miR-133b
hsa-miR-5586-5p
hsa-miR-93-5p
ARHGAP20
ATP1A2
BVES
CCBE1
CD38
CDC42EP3
EYA1
EYA4
HES4
HLF
ITGA2
MKI67
MYOCD
PAK3
PARM1
PRRG4
RGS7BP
SDCCAG3
SLC15A2
SSTR1
STARD4
SYNPO2
TRAF3IP2

Figure 1. lncHUPC1, miR-133b and SDCCAG3 all have differences both in expression and PFS in PCa from TCGA database analysis. A. Heatmap of differentially expressed lncRNA associated with PFS. B. Volcanic plot of differentially expressed lncRNAs. C. Heatmap of differential expressed miRNA which correlated with PFS. D. Volcano plot of differential expressed miRNAs. E. Heatmap of differential expressed mRNA which correlated with PFS. F. Volcano plot of differential expressed mRNAs. G. The alluvial diagram of regulatory network of lncRNA/miRNA/mRNA.

A total of 40 miRNAs were found to be down-regulated and 115 miRNAs were up-regulated (**Figure 1C**). About 29 miRNAs positively were related to PFS and 38 miRNAs negatively related to PFS. Taken together, 16 up-regulated miRNAs negatively associated with PFS (HR > 1, P < 0.01), and 10 down-regulated miRNAs positively associated with PFS (HR < 1, P < 0.01) (**Figure 1D**).

A total of 792 mRNAs were found to be up-regulated and 1230 mRNAs were down-regulated (**Figure 1E**). 2773 mRNAs were negatively related to PFS, and 522 mRNAs were positively related to PFS. To sum up, 103 up-regulated mRNAs negatively correlated with PFS (HR > 1, P < 0.01), and 122 down-regulated mRNAs positively correlated with PFS (HR < 1, P < 0.01) (**Figure 1F**).

LncBase predicted tool was used to predict the targeted miRNAs of lncRNAs, and lncRNAs and miRNAs that were differentially expressed and related to PFS were analyzed. It was identified that the up-regulated lncRNA ENSG00000269131 (lncRNA AC004447.2) was targeted with miR-133b, ENSG00000250508 was targeted with hsa-miR-5586-5p and hsa-miR-106b-5p, and ENSG00000258274 was targeted with hsa-miR-93-5p and hsa-miR-106b-5p. Then, the miRwalk database was used to predict the target mRNAs of miRNAs. Also, only differentially expressed miRNAs and mRNAs associated with PFS were analyzed. Then, the correlations between lncRNA, miRNA and mRNA were analyzed. The correlation coefficient |R| was set to greater than 0.2 and P < 0.05 (**Figure 1G**). Taken together, lncRNA ENSG00000269131-miR-133b-SDCCAG3 (miRNA-mRNA, |R| > 0.4, P < 0.05) was selected as a newly identified ceRNA will be verified empirically in experiment. There were no studies regarding ENSG00000269131 (lncRNA AC004447.2) reported previously, and therefore, we named lncRNA AC004447.2 as lncHUPC1 (Highly Up-regulated in Prostate Cancer 1).

In the 440 PCa cases obtained from the TCGA database (440 PCa tissues and 48 normal prostate tissues), the expression of lncHUPC1 and SDCCAG3 in PCa was significantly higher than that in normal samples (P < 0.0001, **Figure 2A** and **2C**). The expression of miR-133b in PCa was lower than that in normal samples (P < 0.0001, **Figure 2B**). In samples with a higher Gleason score (GS > 7), the expression levels of lncHUPC1 (P = 0.0032, **Figure 2D**) and SDCCAG3 (P < 0.0001, **Figure 2F**) were also higher than those in samples with a lower GS (GS ≤ 7). The high expression of miR-133b appeared in a higher number of samples with lower GS (P < 0.0001, **Figure 2E**). In the same dataset, survival analysis showed that PCa with a high expression of lncHUPC1 (HR = 1.816, 95% CI (1.168-2.823), P = 0.008, **Figure 2G**) and SDCCAG3 (HR = 2.336, 95% CI (1.479-3.688), P < 0.001, **Figure 2I**) had a shorter PFS, while on the contrary, a high expression of miR-133b was associated with a longer PFS (HR = 0.433, 95% CI (0.276-0.680), P < 0.001, **Figure 2H**). In the correlation analysis, lncHUPC1 and miR-133b (r = -0.2949, P < 0.0001, **Figure 2J**), and miR-133b and SDCCAG3 (r = -0.4222, P < 0.0001, **Figure 2L**) were found to be negatively correlated, while lncHUPC1 and SDCCAG3 were found to be positively correlated (r = 0.5316, P < 0.0001, **Figure 2K**).

The differential expression and clinical significance of lncHUPC1/miR-133b/SDCCAG3 in Pca

The q-PCR results confirmed the high expression of lncHUPC1 and SDCCAG3 in the clinical samples (P < 0.05, **Figure 3A** and **3C**), and the expression of miR-133b in PCa tissues was lower than that in adjacent non-tumor tissues (P < 0.05, **Figure 3B**). Similar to the results of the database analysis, in samples with a high GS (GS > 7), the expression levels of lncHUPC1 (P = 0.0007) and SDCCAG3 (P = 0.0032) were also higher than those in samples with a lower score (GS ≤ 7) (**Figure 3D** and **3F**). A high expression of miR-133b was observed in a higher number of samples with lower GS (P = 0.0005, **Figure 3E**). In the correlation analysis, lncHUPC1 and miR-133b (r = -0.3446, P =

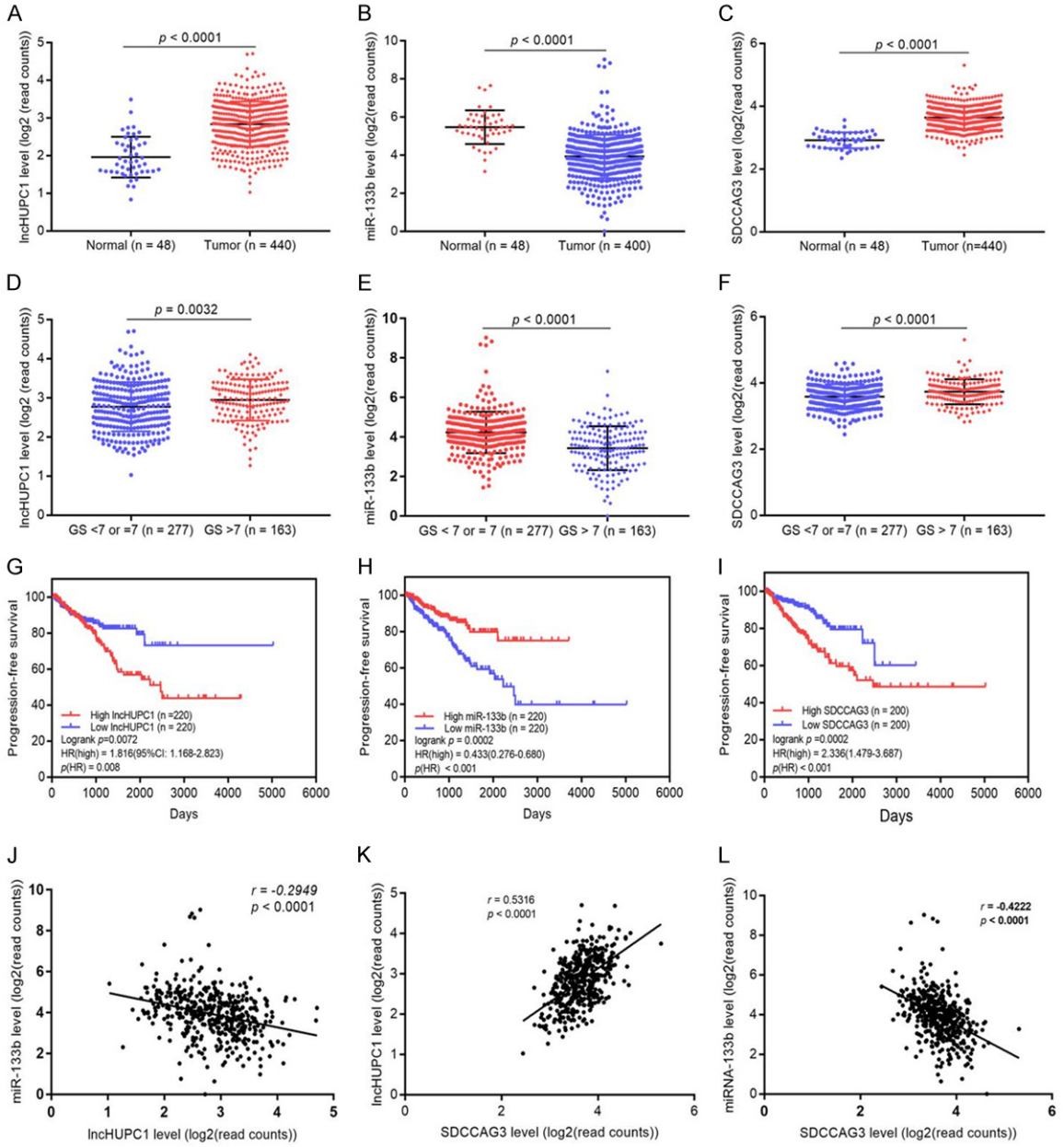

Figure 2. The expression difference, survival analysis and expression correlation of lncHUPC1, miR-133b and SDCCAG3 in PCa in the TCGA database. A, C. The expression levels of lncHUPC1 and SDCCAG3 in PCa were higher than those in normal tissues. B. The expression of miR-133b in PCa was lower than that in normal samples. D, F. The expression levels of lncHUPC1 and SDCCAG3 were higher in samples with a higher Gleason score (GS > 7). E. The high expression of miR-133b appeared in samples with lower Gleason score (GS ≤ 7). G, I. High lncHUPC1 or SDCCAG3 expression indicated poor PFS. H. High miR-133b expression indicated long PFS. J. The relativity between lncHUPC1 and miR-133b. K. The relativity between lncHUPC1 and SDCCAG3. L. The relativity between miR-133b and SDCCAG3.

0.0035, **Figure 3G**), and miR-133b and SDCCAG3 (r = -0.4567, P < 0.0001, **Figure 3H**) were negatively correlated, while lncHUPC1 and SDCCAG3 were positively correlated (r = 0.5064, P < 0.0001, **Figure 3I**). HE and immunohistochemical staining showed that SDCCAG3 was stained positive in tumor tissues and negative in samples of adjacent tissues, and samples with a higher Gleason score showed stronger staining than those with a lower Gleason score (P < 0.05, **Figure 3J** and **3K**). The relative expression of lncHUPC1 in tis-

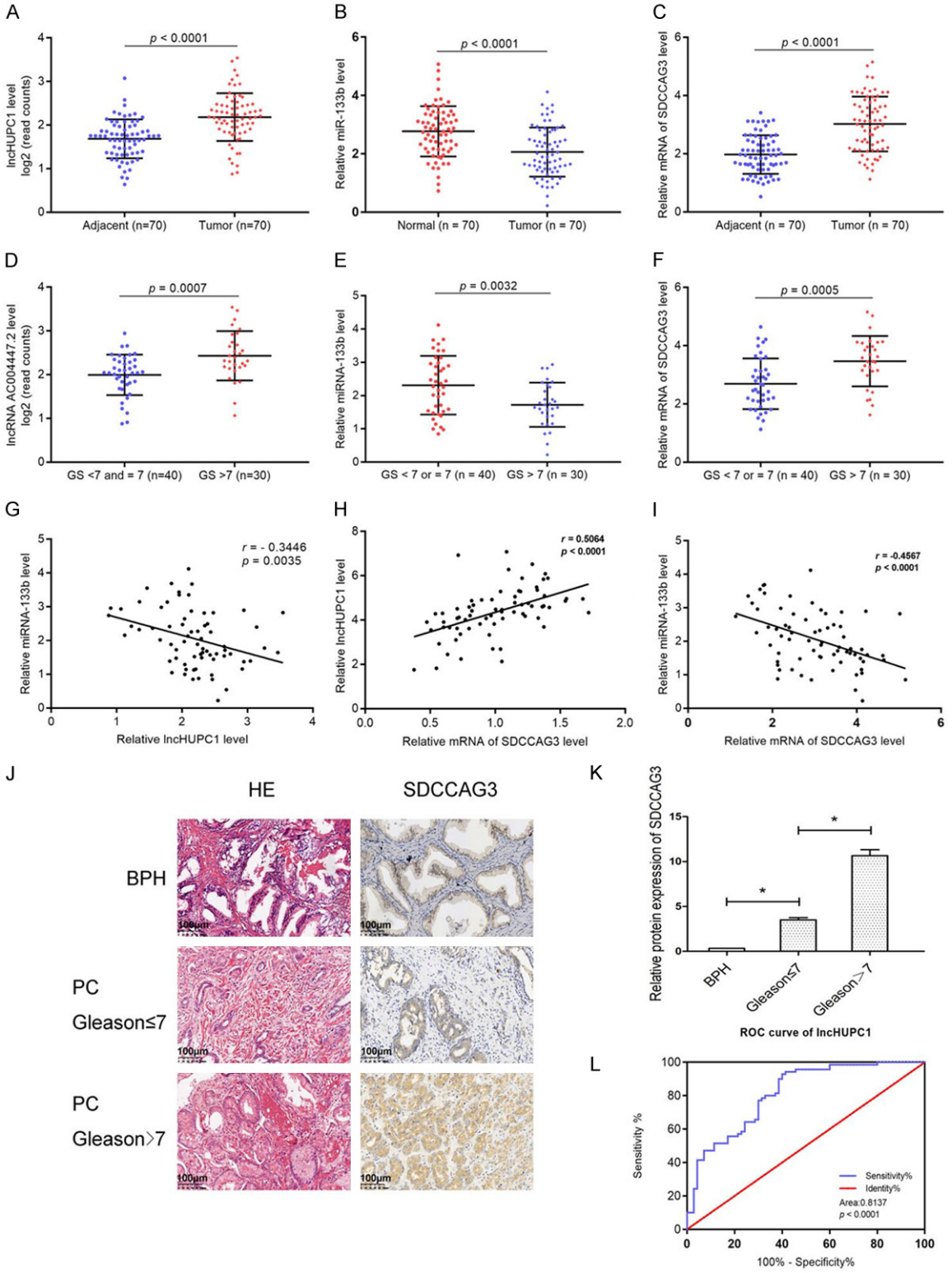

Figure 3. The differential expression and clinical significance of lncHUPC1/miR-133b/SDCCAG3 in PCa. A-C. The expression level of lncHUPC1, miR-133b and SDCCAG3 in PCa tissues and adjacent non-tumor tissues. D-F. The expression level of lncHUPC1, miR-133b and SDCCAG3 in GS ≤ 7 vs GS > 7 in PCa tissues. G. The relativity between lncHUPC1 and miR-133b. H. The relativity between lncHUPC1 and SDCCAG3. I. The relativity between miR-133b and SDCCAG3. J, K. HE and IHC staining showed that SDCCAG3 was stained positive in tumor tissues and negative in samples of adjacent tissues, and samples with a higher Gleason score showed stronger staining than those with a lower Gleason score. L. The AUC curve of lncHUPC1. *P < 0.01.

sues and the diagnosis of PCa in clinical samples form the ROC curve, and the area under the ROC curve (AUC) was 0.955, indicating that lncHUPC1 was a better diagnostic marker of PCa ($P < 0.0001$, **Figure 3L**).

Then, based on the median expression of lncHUPC1 in PCa tissues, patients were categorized into lncHUPC1-high or -low groups to explore the clinical significance of lncHUPC1 in PCa. Tissue analysis showed that a high expression of lncHUPC1 was significantly correlated with a higher GS score ($P = 0.0079$), PSA ($P = 0.0109$), and advanced tumor lymph node metastasis (TNM) stages ($P = 0.0083$) (**Table 1**).

Expression of lncHUPC1/miR-133b/SDCCAG3 in PCa cell lines in vitro and localization of lncHUPC1

In *vitro* experiments were performed using various PCa cell lines (LNCaP, 22RV1, DU145, and PC3) and immortal normal prostate cell line (RWPE-1). The expression levels of lncHUPC1, miR-133b, and SDCCAG3 were measured using q-PCR and western blotting (WB). The q-PCR results showed that lncHUPC1 and SDCCAG3 were highly expressed in PCa cells ($P < 0.05$, **Figure 4A** and **4C**), while miR-133b expression was low in PCa cells ($P < 0.05$, **Figure 4B**). WB results also verified the results for SDCCAG3 (**Figure 4D**). The expression of lncHUPC1 in the nucleus and cytoplasm was analyzed using q-PCR (**Figure 4E**) and FISH probes (**Figure 4F**) by extracting RNA from the nucleus and cytoplasm, respectively. The results of the two experiments showed that lncRNA was mainly expressed in the cytoplasm. The sequence of lncHUPC1 was verified in 22RV1 cells using the 5'RACE and 3'RACE experiments. The primers and sequencing results are shown in Table S1 and **Figure 4G**. The results proved that the total length of the lncHUPC1 sequence was 2924 bp, which was consistent with the UCSC database.

lncHUPC1 helps inhibit PCa cell apoptosis and promote growth in vitro

To study the function of lncHUPC1 in PCa cells *in vitro*, we first used lentivirus-packed plasmids to stably knockdown lncHUPC1 in 22RV1 cells (sh lncHUPC1 vs sh control). The transfection efficiency of the two PCa cell lines in the case of lncHUPC1 knockdown is shown in **Figure 5A** ($P < 0.05$). The CCK-8 and clonogenesis experiment results showed that LNCaP and 22RV1 cells knocked down using lncHUPC1 grew significantly slower than those in the control group ($P < 0.05$, **Figure 5B** and **5C**). Flow cytometry analysis showed that lncHUPC1 deletion significantly induced apoptosis in LNCaP and 22RV1 cells ($P < 0.05$, **Figure 5D** and **5E**). Also, knocking down lncHUPC1 in PCa cells resulted in a significant downregulation in SDCCAG3 and cas8 cleavage of key apoptosis-related proteins, as shown using WB ($P < 0.05$, **Figure 5F**).

lncHUPC1 promotes the growth and metastasis of PCa cells in vivo

The results of *in vitro* experiments showed that lncHUPC1, as an oncogene, is involved in the progression of PCa. To fortify the results, various *in vivo* experiments were conducted to study the effect of lncHUPC1 on the growth and metastasis of PCa cells. The 22RV1 cells transfected with sh lncHUPC1 and sh control group were implanted into nude mice using subcutaneous and tibial injections. The results showed that compared to the sh control group, down-regulating lncHUPC1 in 22RV1 cells significantly inhibited the growth of the subcutaneous tumor cells ($P < 0.05$, **Figure 6A**). The subcutaneous tumor formed in nude mice was dissected, and IHC staining of the lncHUPC1 knockdown group also confirmed that the expression of Ki67 and SDCCAG3 significantly reduced, while that of cleaved cas8 significantly increased ($P < 0.05$, **Figure 6B**). In the bone metastasis mice model, the ratio of bone metastases/whole hind limbs in the sh lncHUPC1 group was lower than that in the sh control group ($P < 0.05$, **Figure 6C**). It was also found that the bone metastases in the nude mice in the sh lncHUPC1 group caused less bone damage than that in the sh control group (**Figure 6D**). HE and IHC staining results showed that the bone destruction by metastases in the sh lncHUPC1 group was less than that in the sh control group, and the expression of cleaved cas8 in bone metastases was significantly increased, as shown using IHC staining ($P < 0.05$, **Figure 6E**).

lncHUPC1 affects the expression of SDCCAG3 through miR-133b

These two kinds (LNCaP and 22RV1) of PCa cells were transfected with sh lncHUPC1 plas-

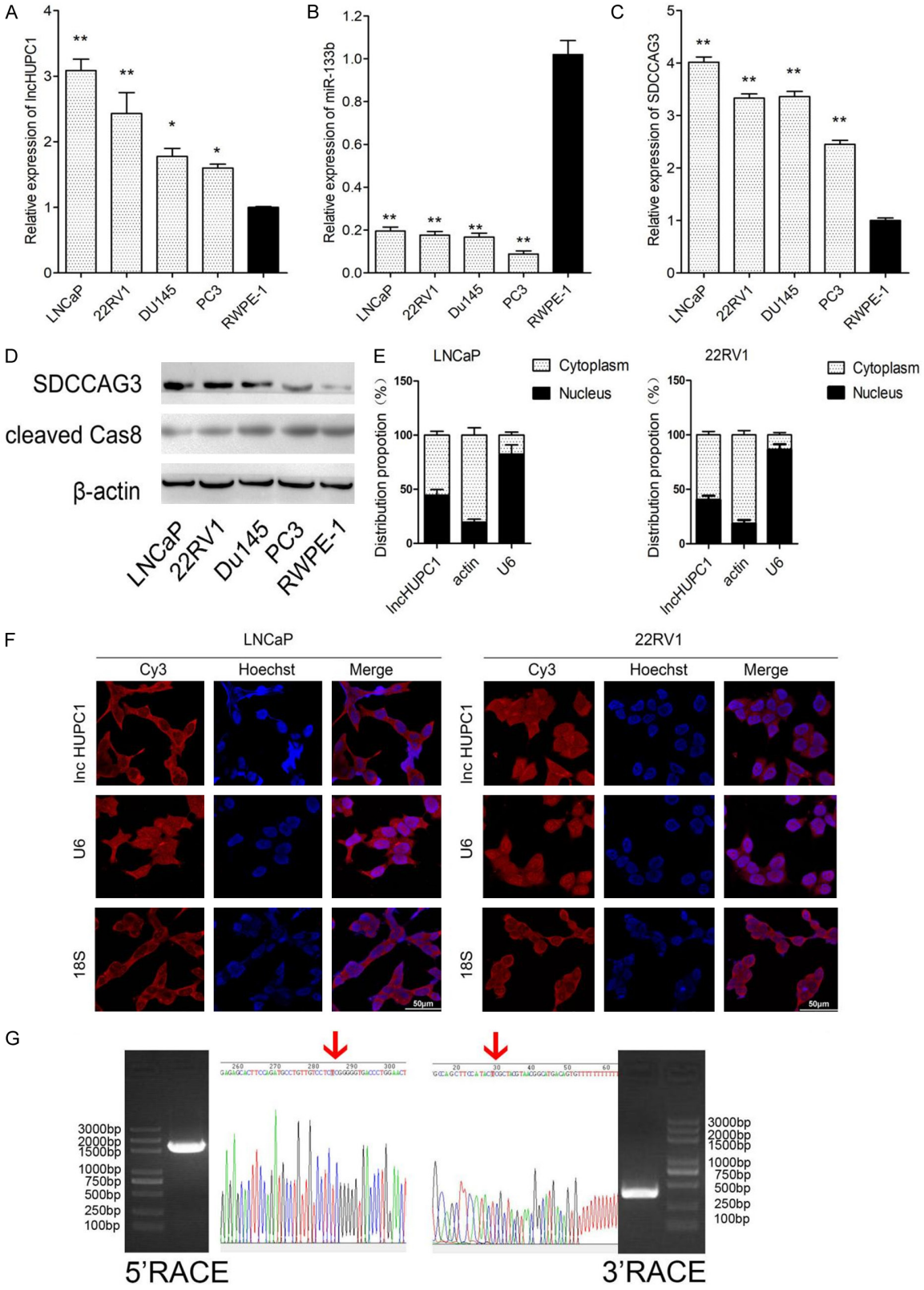

Figure 4. Expression of lncHUPC1/miR-133b/SDCCAG3 in PCa cell lines in vitro and localization of lncHUPC1. A-C. q-PCR results of lncHUPC1, miR-133b and SDCCAG3 expression in PCa and BPH cells, respectively. D. WB results of SDCCAG3 and cleaved Cas8 expression in PCa and BPH cells. E. q-PCR results of nuclear and cytoplasmic RNA isolation was applied to determine lncHUPC1 subcellular localization. F. lncRNA fish probe suggests that lncHUPC1 is mainly expressed in the cytoplasm. G. RACE experiment verifies the full length of lncHUPC1. *P < 0.05, **P < 0.01.

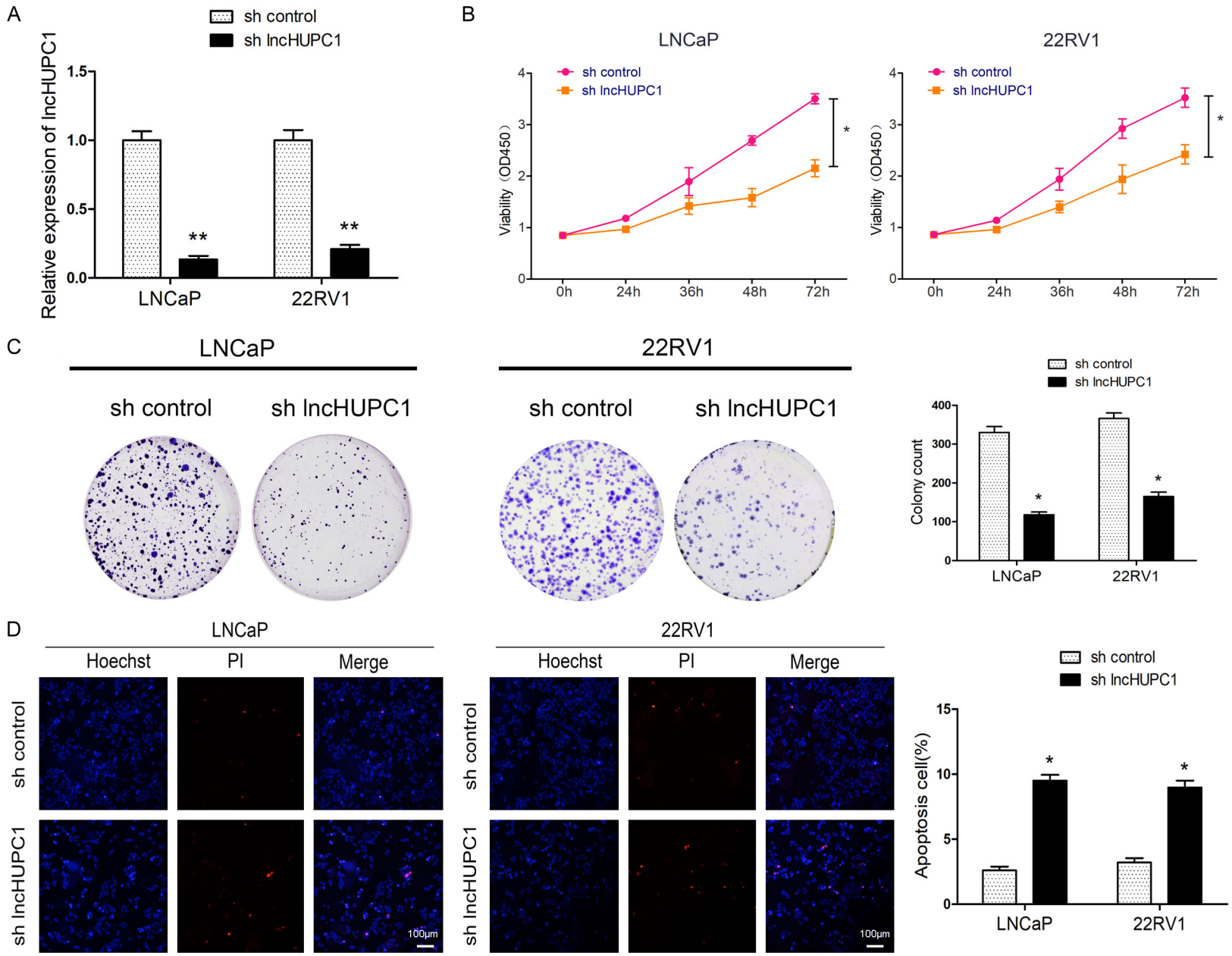
A
sh control
sh lncHUPC1
Relative expression of lncHUPC1
1.5
1.0
0.5
0.0
**
**
LNCaP
22RV1
B
LNCaP
22RV1
sh control
sh lncHUPC1
Viability（OD450）
4
3
2
1
0
0h
24h
36h
48h
72h
*
C
LNCaP
22RV1
sh control
sh lncHUPC1
Colony count
400
300
200
100
0
*
D
LNCaP
22RV1
Hoechst
PI
Merge
sh control
sh lncHUPC1
100μm
Apoptosis cell(%)
15
10
5
0

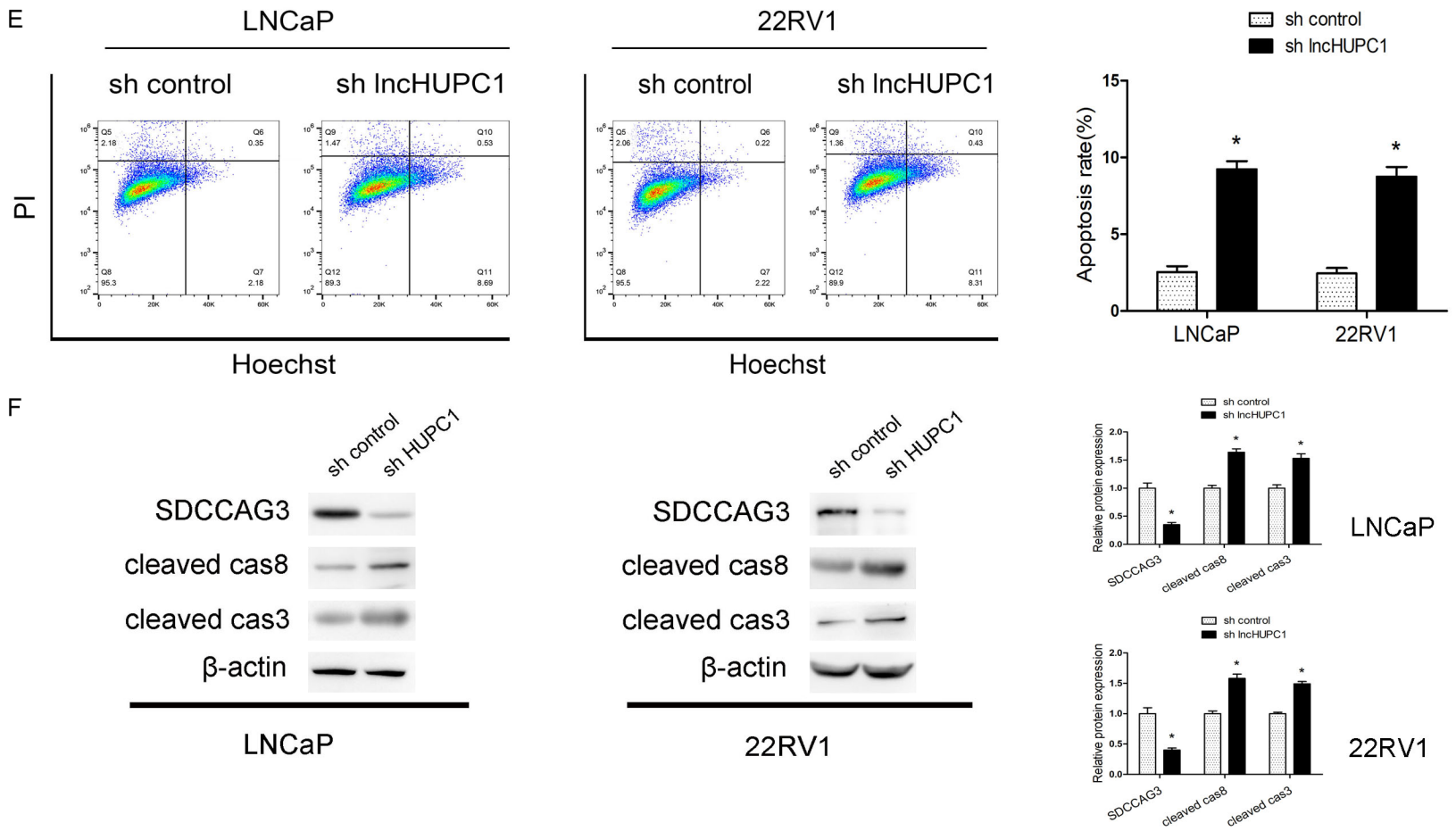

Figure 5. Knockdown of lncHUPC1 reduced proliferation and increased apoptosis. (A) q-PCR validated the efficiency of knocking down lncHUPC1. (B) CCK-8 assay, (C) Clone formation to verify the effect of knockdown lncHUPC1 on cell proliferation. (D) Apoptosis staining and (E) flow cytometry to verify the effect of knockdown of lncHUPC1 on cell apoptosis. (F) WB verified the effect of knocking down lncHUPC1 on the expression of SDCCAG3 and cleaved cas8. *P < 0.05, **P < 0.01.

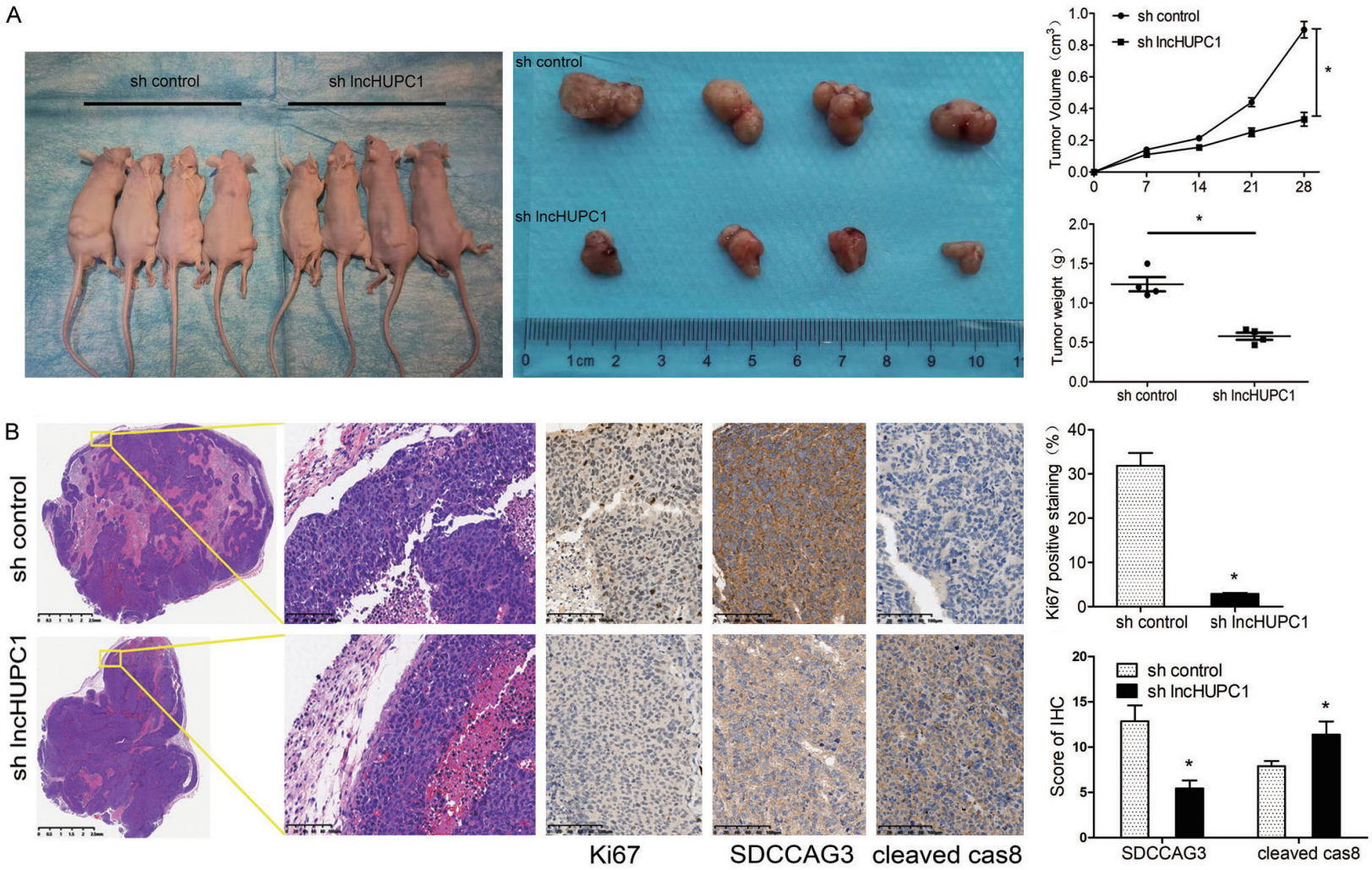
A
sh control
sh lncHUPC1
sh control
sh lncHUPC1
0 1cm 2 3 4 5 6 7 8 9 10 1
sh control
sh lncHUPC1
Tumor Volume (cm3)
1.0
0.8
0.6
0.4
0.2
0.0
0 7 14 21 28
*
Tumor weight (g)
2.0
1.5
1.0
0.5
0.0
*
sh control
sh lncHUPC1
B
sh control
sh lncHUPC1
Ki67
SDCCAG3
cleaved cas8
Ki67 positive staining (%)
40
30
20
10
0
*
sh control
sh lncHUPC1
Score of IHC
20
15
10
5
0
sh control
sh lncHUPC1
*
*
SDCCAG3
cleaved cas8

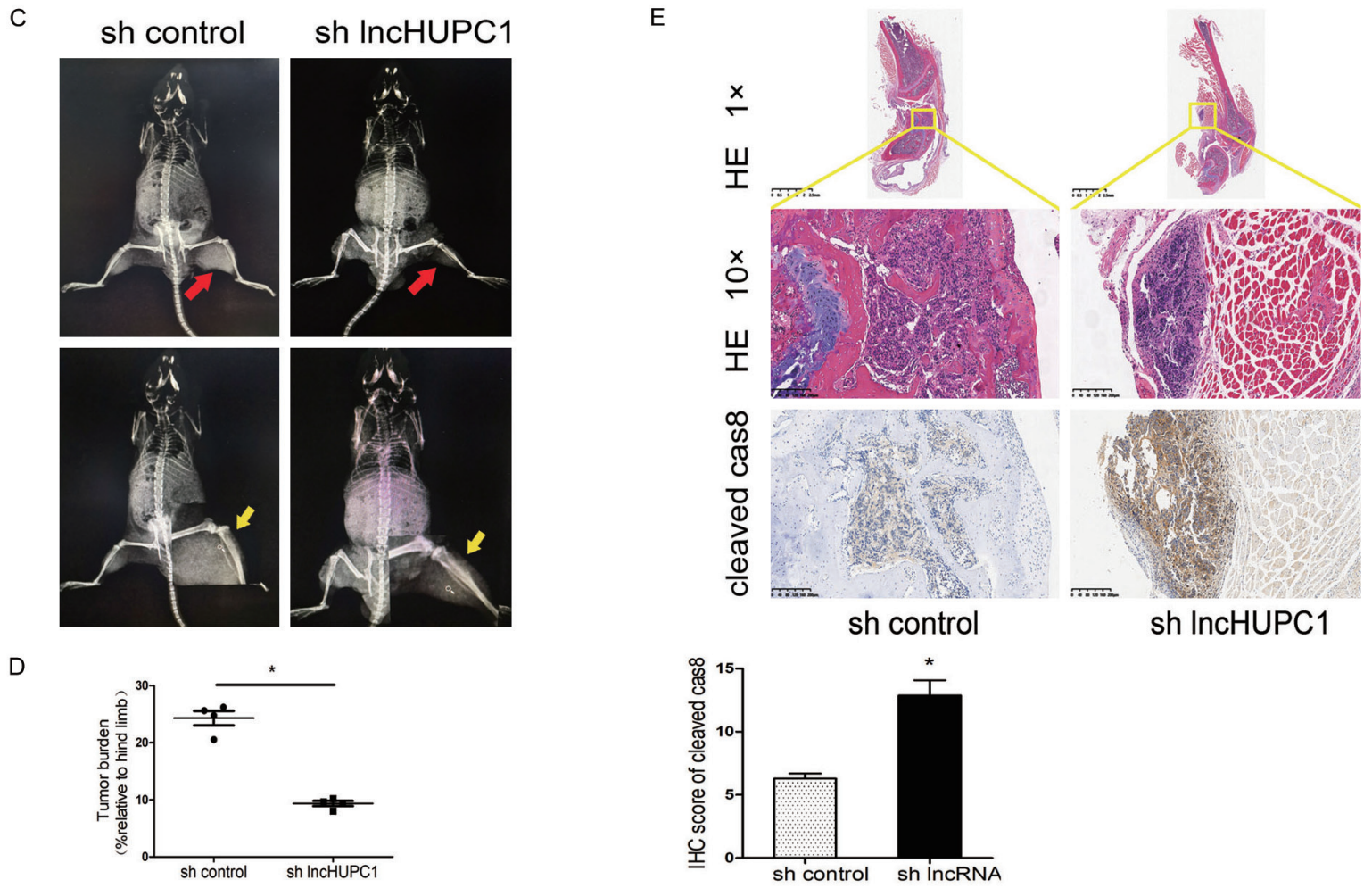

Figure 6. lncHUPC1 promotes proliferation and inhibits apoptosis of PCa cell in vivo. A. Xenograft tumor formation experiments confirmed that knocking down lncHUPC1 affects tumor size and growth rate in nude mice. B. IHC results of Ki67, SDCCAG3 and cleaved Cas8 for xenograft tumors. C. X-rays of the bone metastasis in mice hind leg. The red arrow points to the bone graft tumor. The yellow arrow points to the site of bone destruction caused by the tumor. D. Proportion of weight of bone metastases to hind limbs. E. HE and IHC results of bone metastasis. *$P < 0.05$.

mid packaged by lentivirus, along with mimic and inhibitor of miR-133b. An empty virus plus blank control sequence group (sh control + miR NC), lncHUPC1 knockdown plus miRNA blank control group (sh lncHUPC1 + miR NC), lncHUPC1 and miR-133b simultaneous knockdown group (sh lncHUPC1 + miR-133b inhibitor), and lncHUPC1 knockdown and miR-133b overexpression group (sh lncHUPC1 + miR-133b mimic) were created. Compared to the sh control + miR NC group, the sh lncHUPC1 + miR NC, lncHUPC1 + miR-133b inhibitor, and lncHUPC1 + miR-133b mimic groups showed the same degree of decrease in lncHUPC1 ($P < 0.05$, **Figure 7A**). The expression of miR-133b in the sh lncHUPC1 + miR NC group was significantly higher than that in the sh lncHUPC1 + miR NC group, while miR-133b in the sh lncHUPC1 + miR-133b inhibitor group showed some decrease. The expression of miR-133b in the sh lncHUPC1 + miR-133b mimic group was the highest among the 4 groups, and the result was significant ($P < 0.05$, **Figure 7B**). The expression of SDCCAG3 mRNA decreased in the sh lncHUPC1 + miR NC group compared to the sh control + miR NC group, and the expression of SDCCAG3 increased after adding miR-133b inhibitor in the sh lncHUPC1 + miR-133b inhibitor group. The expression of SDCCAG3 in the sh lncHUPC1 + miR-133b mimic group was the lowest among the 4 groups ($P < 0.05$, **Figure 7C**). WB results confirmed that knock down of lncHUPC1 reduced the expression of SDCCAG3 and increased that of cleaved caspase8 and cleaved caspase3, activating the apoptotic pathway. When the expression of lncHUPC1 and miR-133b was reduced at the same time (sh lncHUPC1 + miR-133b inhibitor group), the expression of SDCCAG3 partially increased, and that of cleaved caspase8 partially reduced. Decreasing the expression of lncHUPC1 and increasing the expression of miR-133b can significantly reduce the expression of SDCCAG3 and increase that of cleaved caspase8 ($P < 0.05$, **Figure 7D**).

The biological function of ceRNA of lncHUPC1/miR-133b/SDCCAG3

To investigate whether lncHUPC1 affected the growth and apoptosis of PCa cells through miR-133b/SDCCAG3 forming a ceRNA network, we conducted the following experiments. The results of the CCK-8 and colony formation experiments showed that miR-133b inhibitors can partially reverse the anti-proliferative and apoptotic effects of sh lncHUPC1, while miR-133b mimic enhanced these effects and decreased the proliferation ability of the cells and enhanced apoptosis ($P < 0.05$, **Figure 8A** and **8B**). In addition, the results of flow cytometry and Hoechst/PI *in situ* staining showed that co-transfection with miR-133b inhibitors can inhibit the apoptosis induced by the downregulation of lncHUPC1, while miR-133b mimic can enhance the effect of lncHUPC1 on cell apoptosis ($P < 0.05$, **Figure 8C** and **8D**).

miR-133b bounds with lncHUPC1

Firstly, we predicted the binding sites of lncHUPC1 3'UTR and miRNA 5'UTR using Targetscan and RNAhybrid databases (**Figure 9A**). q-PCR results again verified that knocking down lncHUPC1 increased the expression of miR-133b ($P < 0.05$, **Figure 9B**). Luciferase assay results showed that miR-133b mimics decreased luciferase activity in vectors containing wild-type lncHUPC1 (wt) but failed to decrease luciferase activity in vectors containing lncHUPC1 mutation (mut), suggesting that miR-133b may directly bind to lncHUPC1 ($P < 0.05$, **Figure 9C**). We, then, performed the ChIRP assay to determine the direct interaction between lncHUPC1 and miR-133b. To improve the specificity of ChIRP detection, 5 oligonucleotide probes targeting lncHUPC1 were designed and divided into even and odd groups. Results confirmed that miR-133b was adsorbed by lncHUPC1 significantly in even and odd probe pools compared to control LacZ probes set in LNCaP and 22RV1 cells ($P < 0.05$, **Figure 9D**).

SDCCAG3 was the direct target of miR-133b

The Targetscan database was used to predict the binding sites of SDCCAG3 3'UTR and miR-133b 5'UTR (**Figure 9E**). The results of q-PCR and WB confirmed that the mRNA and protein expression of SDCCAG3 decreased after transcription of miR-133b mimic ($P < 0.05$, **Figure 9F** and **9G**). The results of the luciferase assay showed that miR-133b mimic can significantly negatively regulate the luciferase activity of the wild-type SDCCAG3 mRNA vector (wt) but cannot reduce the luciferase activity of the mutant vector (mut) ($P < 0.05$, **Figure 9H**),

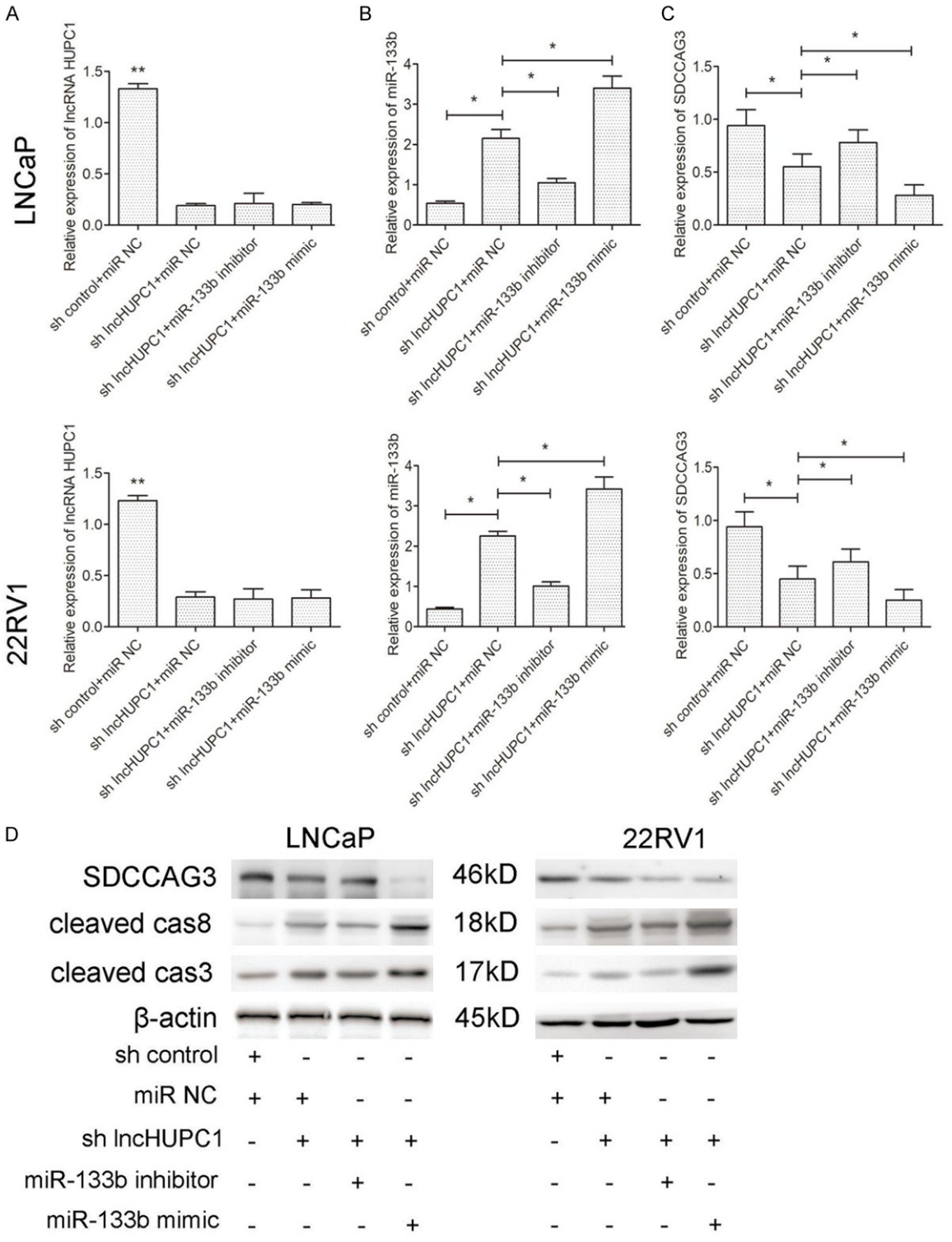

Figure 7. lncHUPC1 affects the expression of SDCCAG3 through miR-133b. (A) Compared with the sh control + miR NC group, the sh lncHUPC1 + miR NC, lncHUPC1 + miR-133b inhibitor, and lncHUPC1 + miR-133b mimic groups showed the same degree of decrease in lncHUPC1. (B) The expression of miR-133b, (C) SDCCAG3 in PCa cells transfected with sh lncHUPCA or miR-133b inhibitor or miR-133b mimic compared to their negative controls. (D) The changes of SDCCAG3 protein expression in each treatment group were demonstrated by WB results. *P < 0.05, **P < 0.01.

A

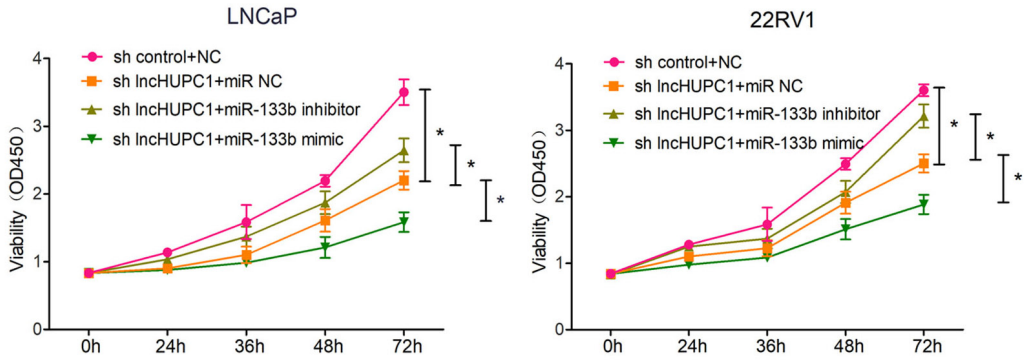
LNCaP
22RV1
sh control+NC
sh lncHUPC1+miR NC
sh lncHUPC1+miR-133b inhibitor
sh lncHUPC1+miR-133b mimic
Viability（OD450）
0h
24h
36h
48h
72h

B

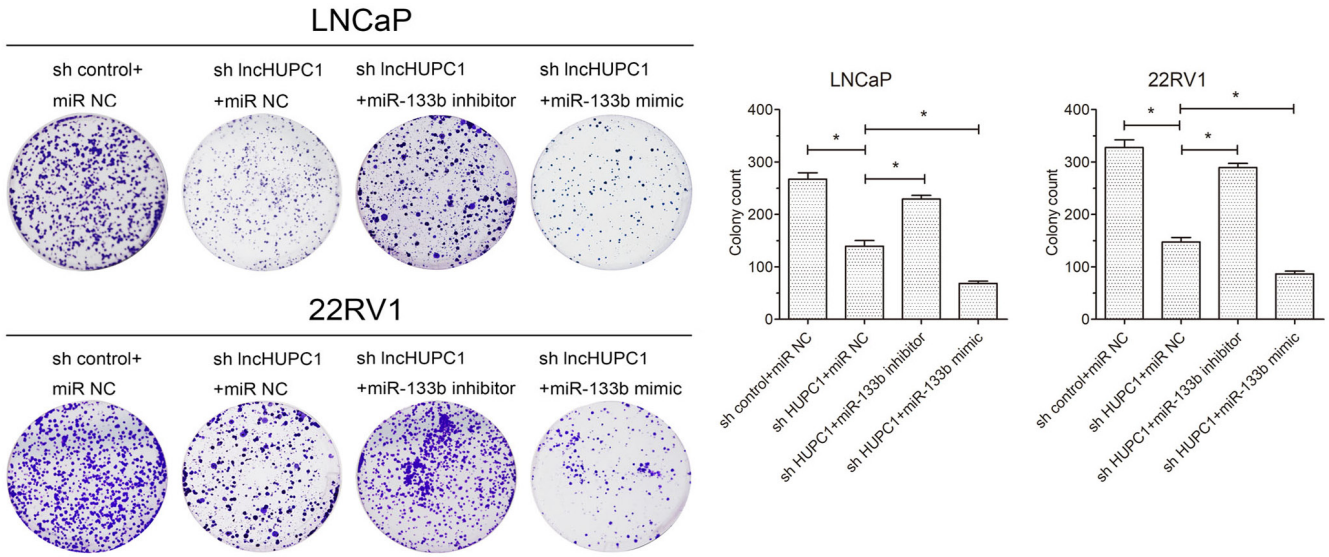
LNCaP
sh control+ miR NC
sh lncHUPC1 +miR NC
sh lncHUPC1 +miR-133b inhibitor
sh lncHUPC1 +miR-133b mimic
22RV1
LNCaP
22RV1
Colony count
sh control+miR NC
sh HUPC1+miR NC
sh HUPC1+miR-133b inhibitor
sh HUPC1+miR-133b mimic

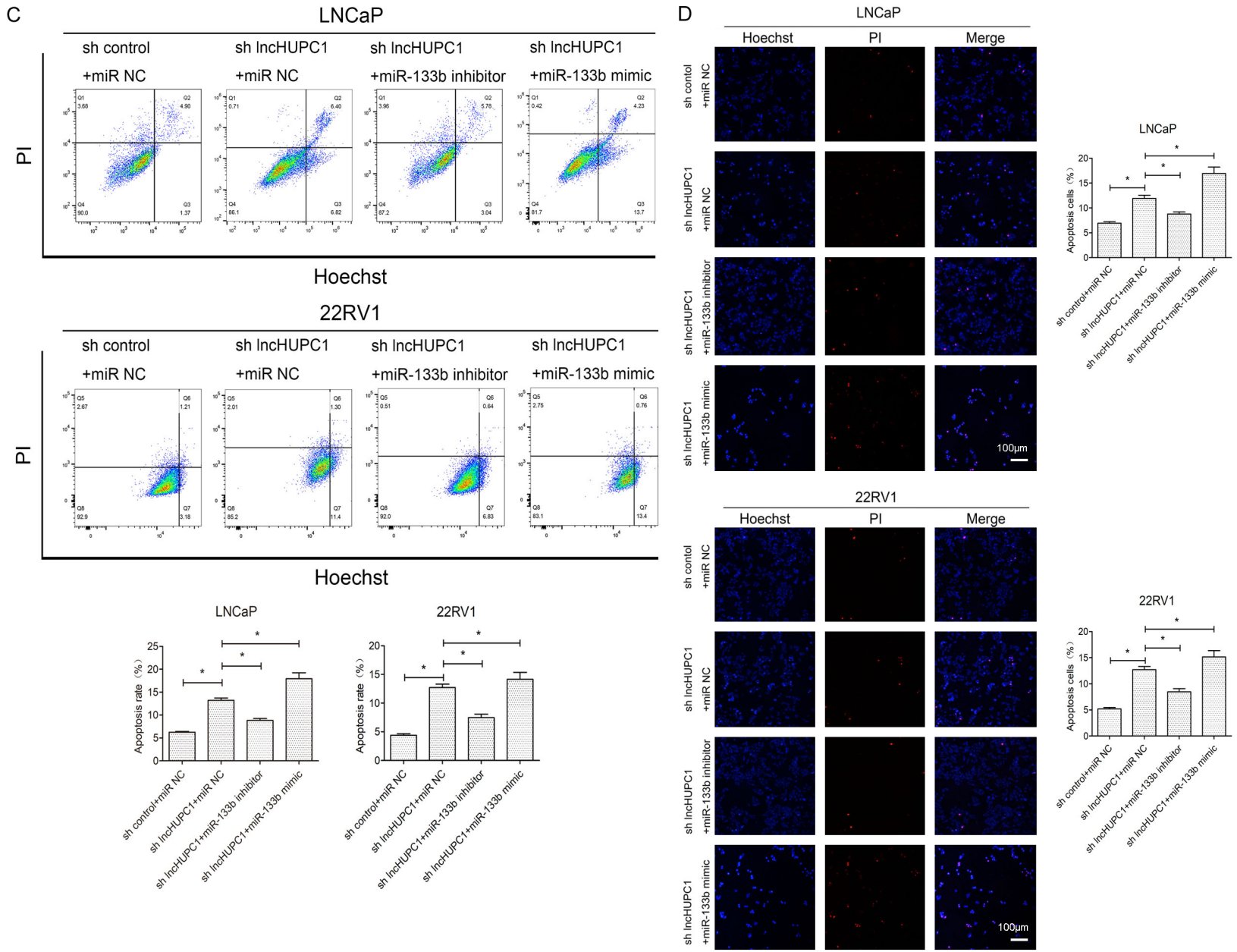
C
LNCaP
sh control +miR NC
sh lncHUPC1 +miR NC
sh lncHUPC1 +miR-133b inhibitor
sh lncHUPC1 +miR-133b mimic
PI
Hoechst
22RV1
Apoptosis rate (%)
sh control+miR NC
sh lncHUPC1+miR NC
sh lncHUPC1+miR-133b inhibitor
sh lncHUPC1+miR-133b mimic
D
Hoechst
PI
Merge
100μm
Apoptosis cells (%)

Figure 8. Biological function of ceRNA of lncHUPC1/miR-133b/SDCCAG3. (A) The CCK-8 assays, (B) colony formation experiments showed that miR-133b inhibitors can partially reverse the anti-proliferative and apoptotic effects of sh lncHUPC1, while miR-133b mimic enhanced these effects and decreased the proliferation ability of the cells. the results of (C) flow cytometry, (D) Hoechst/PI *in situ* staining showed that co-transfection with miR-133b inhibitors can inhibit the apoptosis induced by the downregulation of lncHUPC1, while miR-133b mimic can enhance the effect of lncHUPC1 on cell apoptosis. *P < 0.05.

indicating that miR-133b can directly bind to SDCCAG3 mRNA.

FOXA1 regulates the lncHUPC1/miR-133b/SDCCAG3 signaling loop

Several studies have confirmed that FOXA1 plays a key role in the occurrence and progression of PCa. According to the analysis of the predicted results by the animal TFDB and JASPAR databases, FOXA1 may bind to the promoter sequence of lncHUPC1 as a transcription factor (**Figure 10A-D**). Knockdown of FOXA1 using plasmid transfection and evaluation using WB showed that SDCCAG3 was significantly reduced in the cells (P < 0.05, **Figure 10E**). It was verified again, using WB, that the knockdown of lncHUPC1 reduced the expression of SDCCAG3 (P < 0.05, **Figure 10F**). However, there was no change in FOXA1, miR-133b, and lncHUPC1 levels after SDCCAG3 was knocked down (P < 0.05, **Figure 10G**). We established a luciferase reporter vector containing lncHUPC1 promoter that overexpressed transcription factor FOXA1. The results showed that the transcription factor FOXA1 positively regulated the promoter of lncHUPC1, and the luciferase activity was reversed by knocking down the promoter of lncHUPC1 (P < 0.05, **Figure 10H**). In addition, ChIP-PCR analysis further confirmed the direct binding of FOXA1 to the promoter of lncHUPC1 (P < 0.05, **Figure 10I**).

These results indicated that FOXA1 can directly bind to the DNA promoter of lncHUPC1 to activate transcription of lncHUPC1, and miR-133b and SDCCAG3 are downstream target genes regulated by lncHUPC1. In short, the FOXA1/lncHUPC1/miR-133b/SDCCAG3 pathway functions in PCa.

Discussion

In recent years, a large number of lncRNAs and miRNAs have been identified to be closely related to the growth and progression of PCa. Several studies have confirmed that lncRNA constitutes a large proportion of miRNA in the cell (mainly in the cytoplasm), and can buffer and reduce the miRNA's ability to degrade target gene mRNA and interfere with the translation process like a "sponge". Therefore, the association of lncRNA and mRNA becomes the ceRNA network through these related points miRNA [16, 17]. Specifically, miRNAs can target and bind to the corresponding mRNA through the guide RNA-induced silencing complex (RISC), resulting in mRNA degradation or post-translational inhibition, leading to the downregulation of the expression of the corresponding protein [18]. A few studies have shown that PCA3 (prostate cancer antigen-3) lncRNA is a prostate-specific lncRNA, which can be used for the early diagnosis of prostate cancer, and has higher specificity and sensitivity compared to PSA [7]. In addition, lncRNA UCA1 also promotes the progression of PCa by regulating the ceRNA of AFT2 [17].

Through the integration of bioinformatics data, we found a sponge regulatory network of lncRNA-mediated targeting of protein-encoding driver genes in PCa-related databases, namely lncRNA AC004447.2/miR-133b/SDCCAG3. The lncRNA AC004447.2, miR-133b, and SDCCAG3 in the ceRNA network were related to the progression of PCa and had a survival impact (PFS) in PCa. Since this particular lncRNA had not been reported previously and is highly expressed in PCa, we named it lncHUPC1. In addition, we found that the expression of miR-133b and lncHUPC1 and that of miR-133b and SDCCAG3 were negatively correlated, while that of lncHUPC1 and SDCCAG3 was positively correlated.

lncHUPC1 acted as a tumor promoter by promoting the growth and metastasis of PCa cells both *in vitro* and *in vivo*. The current study confirmed the carcinogenic effect of lncHUPC1 in PCa for the first time. The subcellular localization of lncRNA could revealed the regulatory mechanism underlying its function. In particu-

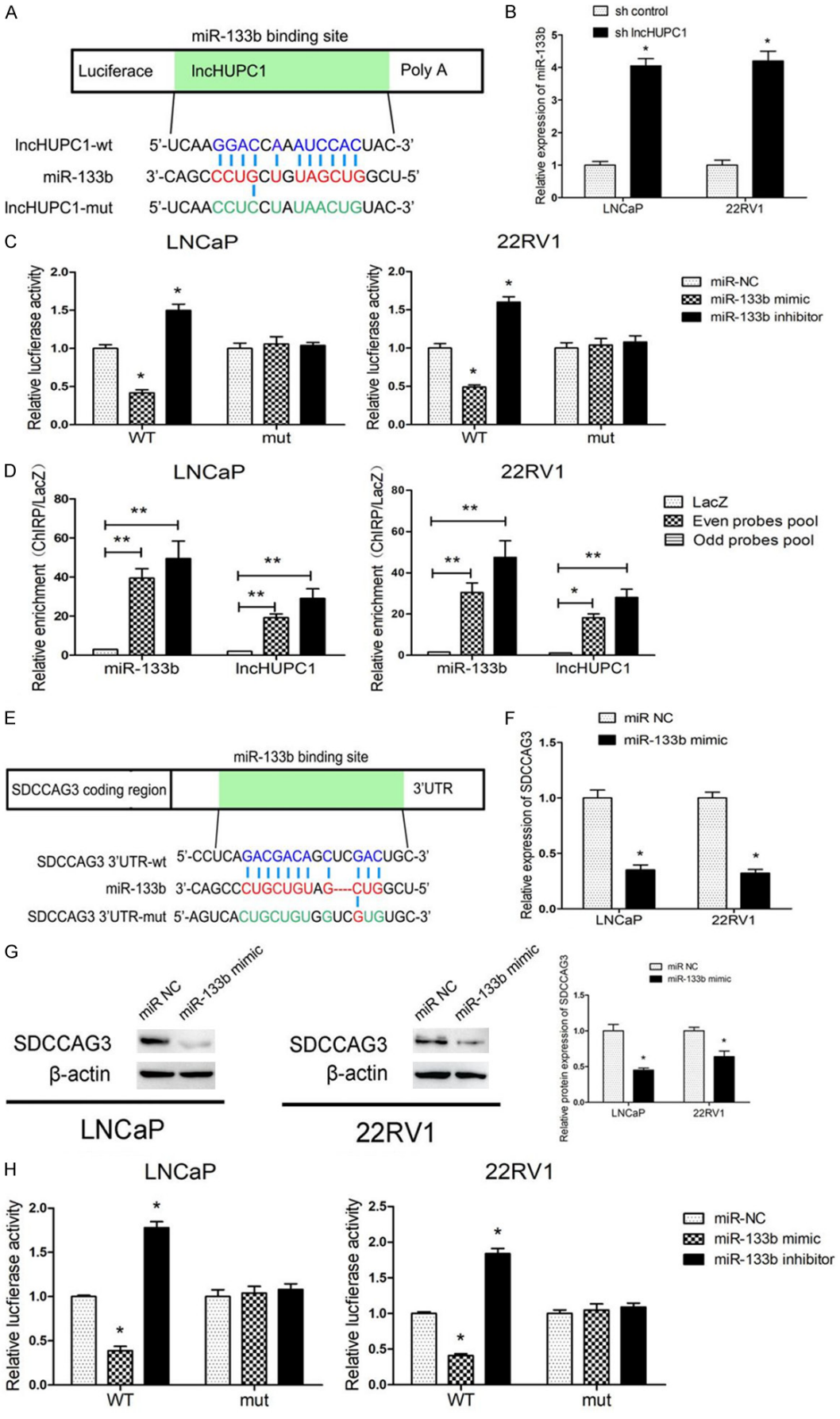
A
miR-133b binding site
Luciferace
lncHUPC1
Poly A
lncHUPC1-wt 5'-UCAAGGACCAAAUCCACUAC-3'
miR-133b 3'-CAGCCCUGCUGUAGCUGGCU-5'
lncHUPC1-mut 5'-UCAACCUCCUAUAACUGUAC-3'
B
sh control
sh lncHUPC1
Relative expression of miR-133b
LNCaP
22RV1
C
LNCaP
22RV1
Relative luciferase activity
WT
mut
miR-NC
miR-133b mimic
miR-133b inhibitor
D
LNCaP
22RV1
Relative enrichment (ChIRP/LacZ)
miR-133b
lncHUPC1
LacZ
Even probes pool
Odd probes pool
E
miR-133b binding site
SDCCAG3 coding region
3'UTR
SDCCAG3 3'UTR-wt 5'-CCUCAGACGACAGCUCGACUGC-3'
miR-133b 3'-CAGCCCUGCUGUAG----CUGGCU-5'
SDCCAG3 3'UTR-mut 5'-AGUCACUGCUGUGGUCGUGUGC-3'
F
miR NC
miR-133b mimic
Relative expression of SDCCAG3
LNCaP
22RV1
G
miR NC
miR-133b mimic
SDCCAG3
β-actin
LNCaP
22RV1
Relative protein expression of SDCCAG3
H
LNCaP
22RV1
Relative luciferase activity
WT
mut
miR-NC
miR-133b mimic
miR-133b inhibitor

Figure 9. lncHUPC1 could directly bind to miR-133b, and miR-133b could directly bind to mRNA of SDCCAG3. A. Predicted binding sites between miR-133b and lncHUPC1 and mutation sequences of potential binding sites of miR-133b in lncHUPC1. B. Expression changes of miR-133b after knockdown of lncHUPC1. C. The result of luciferase reporter assay suggested that lncHUPC1 may directly bind to miR-133b. D. The ChIRP assay determined the direct interaction between lncHUPC1 and miR-133b. E. Predicted binding sites between miR-133b and SDCCAG3 and mutation sequences of potential binding sites of miR-133b in SDCCAG3. F. q-PCR results showed expression changes of SDCCAG3 after overexpression of miR-133b. G. WB showed expression changes of SDCCAG3 protein after overexpression of miR-133b. H. The result of luciferase reporter assay suggested that miR-133b may directly bind to the mRNA of SDCCAG3. *P < 0.05.

lar, lncRNAs located in the cytoplasm generally regulate gene expression at the post-transcriptional level through the ceRNA mechanism [19-21]. In the current study, we observed, using subcytoplasmic separation experiments, that lncHUPC1 was mainly located in the cytoplasm, suggesting that lncHUPC1 may play a carcinogenic role in PCa by acting as a miRNA sponge. The expression of lncHUPC1 and SDCCAG3 was positively correlated in PCa tissue. We proved through a series of repeated experiments that miR-133b mediated the carcinogenic function of lncHUPC1 in PCa cells. In conclusion, we determined that lncHUPC1 could adsorb miR-133b in the cytoplasm of PCa cells.

It has been reported that SDCCAG3 is an endosome-related protein involved in cell division and the regulation of the late fusion of endosomes and lysosomes. In previous studies, in colon cancer cells, SDCCAG3 and PTPN13 formed a complex, which was involved in regulating cell division and reducing apoptosis [8]. The activated Fas formed FADD trimers and gradually transferred from endosomes to lysosomes, thereby activating caspase8, causing the activation of downstream caspase3 and 7, and leading to cell apoptosis. SDCCAG3 binds to PTPN13 and Dysbindin and competes for the binding site of FADD on the lysosome, leading to the termination of the apoptosis signal and promoting cell proliferation [22]. Through bioinformatics prediction and experimental verification, we determined that SDCCAG3 was the direct target of miR-133b in PCa cells. We also conducted a series of knockdown and overexpression experiments to prove that lncHUPC1 promoted the expression of SDCCAG3 in PCa through absorption of miR-133b.

Next, we used the TRlnc database to predict transcription factors that bind to the lncHUPC1 promoter (**Figure 9A**), and then analyzed the scores of the transcription factors using the JASPAR website (**Figure 9B**). Finally, FOXA1 was identified as the transcription factor with the highest score. In PCa, FOXA1 was considered to be the pioneer of HOXB13 and androgen receptor (AR) binding [23]. In addition to playing a role in the AR signaling pathway, FOXA1 could also regulate the expression of genes involved in cell cycle regulation in PCa. FOXA1 could also inhibit the migration of cancer cells and their transition from epithelial cells to mesenchymal cells (epithelial-to-mesenchymal transition, EMT) through the AR-independent pathway [24]. A few clinical studies have concluded that FOXA1 expression was a sign of poor prognosis of prostate cancer, and high FOXA1 levels were associated with a shorter PSA re-elevation or PCa survival [25, 26]. In the current study, we first explored the effect of FOXA1 on the expression of lncHUPC1. We confirmed the regulatory effect of FOXA1 on lncHUPC1 transcription using ChIP and dual-luciferase reporter gene detection. Our results showed that the expression of lncHUPC1 and SDCCAG3 induced by FOXA1 knockdown was significantly reduced. Knockout of lncHUPC1 and SDCCAG3 had no significant effect on the expression of FOXA1. These results indicated that FOXA1, as a transcription factor, can directly bind to the lncHUPC1 promoter and activate its transcription. FOXA1 promoted the expression of lncHUPC1 via the FOXA1/lncHUPCA1/miR-133b/SDCCAG3 signaling pathway in Pca (**Figure 11**).

In summary, by analyzing the data from the TCGA database, we identified a novel ceRNA network, lncHUPC1/miR-133b/SDCCAG3, which enhanced PCa growth and proliferation and reduced apoptosis. Our *in vivo* and in vitro experiments showed that lncHUPC1 regulated the growth of PCa cells via the miR-133b/SDCCAG3 axis and FOXA1 was used as a transcription factor to regulate the transcription of lncHUPC1. These results suggested that lncHUPC1 is a potential novel therapeutic target and prognostic predictor for PCa.

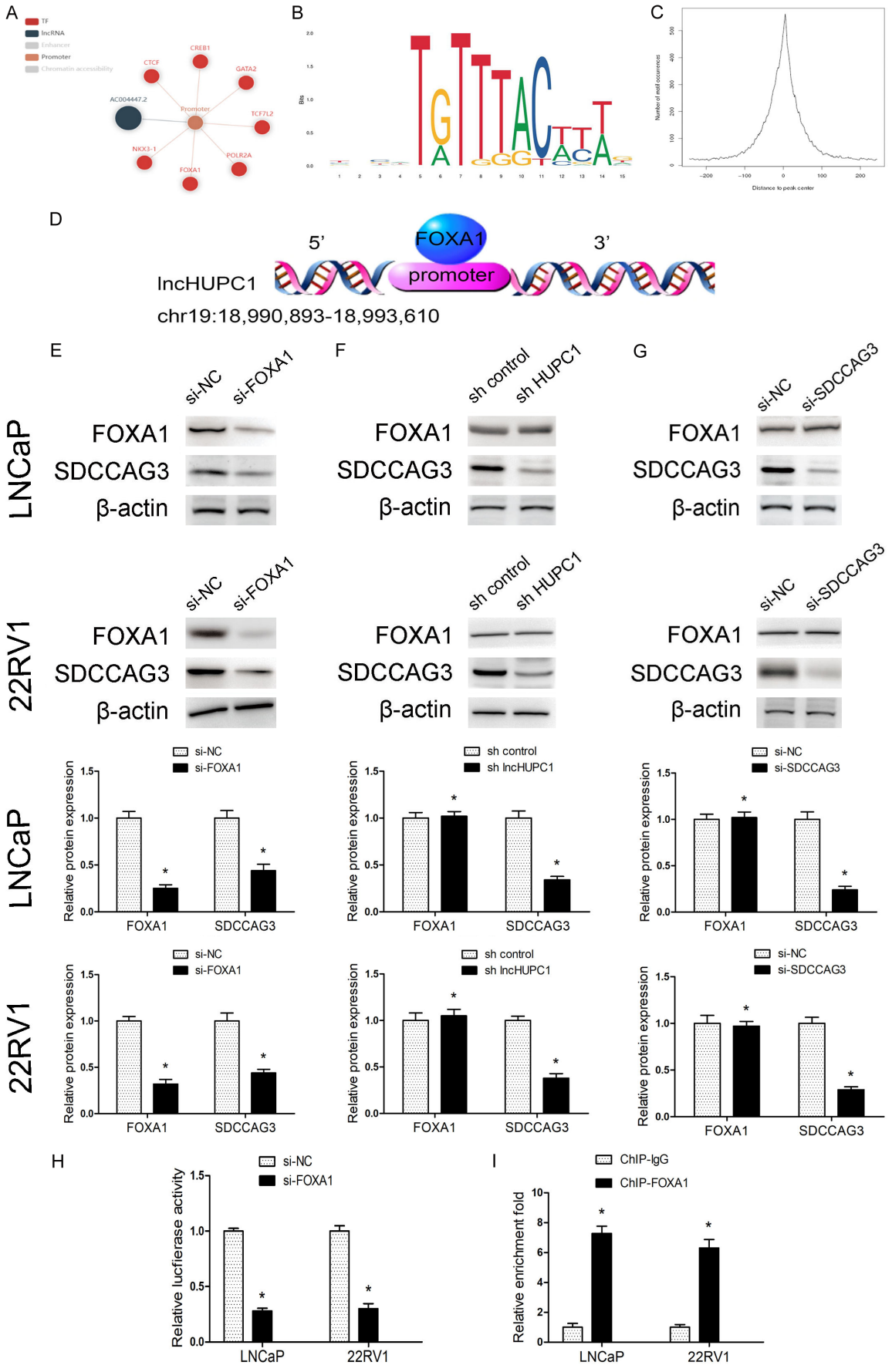
A
TF
lncRNA
Enhancer
Promoter
Chromatin accessibility
CREB1
CTCF
GATA2
AC004447.2
Promoter
TCF7L2
NKX3-1
POLR2A
FOXA1
B
Bits
C
Number of motif occurrence
Distance to peak center
D
5'
FOXA1
3'
lncHUPC1
promoter
chr19:18,990,893-18,993,610
E
si-NC
si-FOXA1
LNCaP
FOXA1
SDCCAG3
β-actin
F
sh control
sh HUPC1
G
si-SDCCAG3
22RV1
Relative protein expression
sh lncHUPC1
H
Relative luciferase activity
I
ChIP-IgG
ChIP-FOXA1
Relative enrichment fold

Figure 10. FOXA1 regulate a lncHUPC1/miR-133b/SDCCAG3 signaling loop. (A) Prediction of transcription factors that promote lncHUPC1 transcription in TRlnc database. (B) The possible binding base sites of lncHUPC1 promoter to FOXA1 were predicted in JASPAR. (C) Motif enrichment results were obtained by ChIP-seq in JASPAR. (D) FOXA1 may be associated with the promoter region of lncHUPC1. After (E) knocking down of FOXA1, (F) knocking down of lncHUPC1, (G) knocking down of SDCCAG3, changes in protein expression levels of FOXA1 and SDCCAG3 in the cells. (H) The luciferase reporter assay exhibited FOXA1 binding to lncHUPC1 promoter. (I) The enrichment of FOXA1 in lncHUPC1 promoter region relative to IgG was analyzed by ChIP. *P < 0.05.

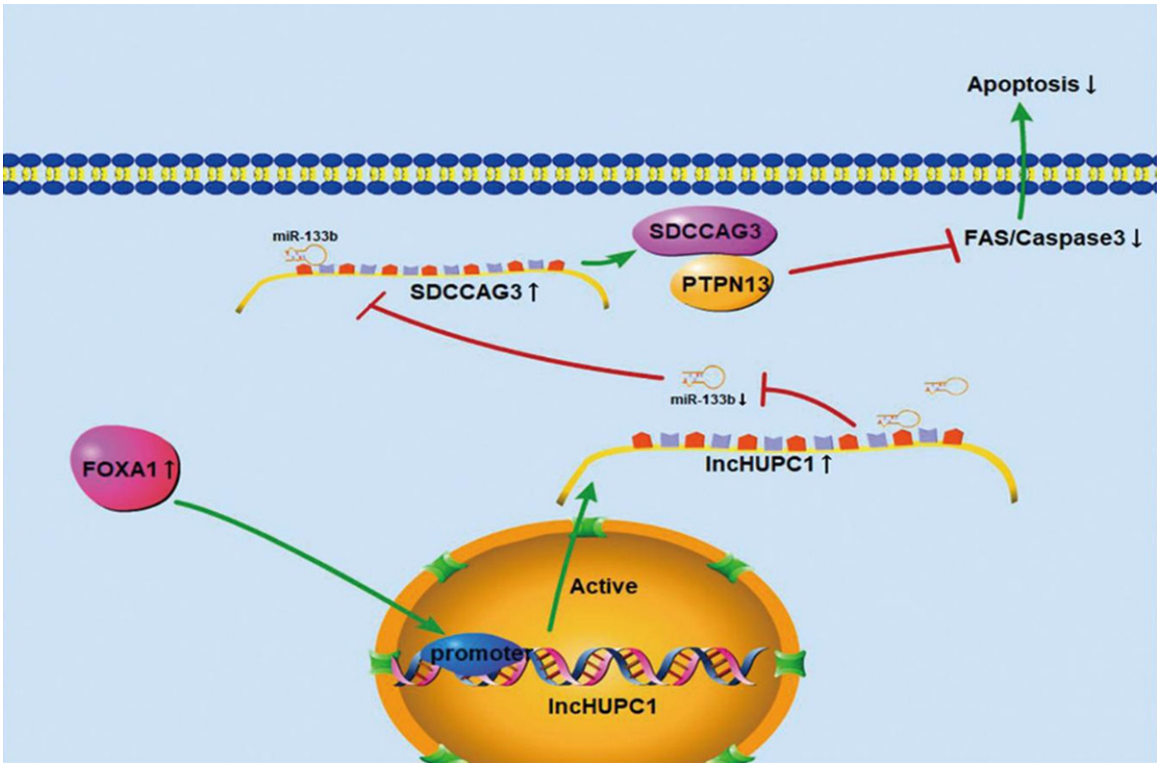

Figure 11. Schematic diagram of the results of this study.

Acknowledgements

This study was supported by grants from Technical Innovation and Application Development Project of Chongqing Science and Technology Bureau (cstc2019jscx-msxmX0144 and cstc2018jscx-msybx0157), Natural Science Foundation of Chongqing municipality (cstc2018jxj1130018) and the Fundamental Research Funds for the Central Universities (No.2021CDJYGRH-015).

Disclosure of conflict of interest

None.

Address correspondence to: Xiaohou Wu, Department of Urology, The First Affiliated Hospital of Chongqing Medical University, Youyi Road 1#, Yuzhong District, Chongqing 400030, China. Tel: +86-023-68811360; E-mail: wuxiaohou2019@163.com; Hao Sun, Gastrointestinal Cancer Center, Chongqing University Cancer Hospital, Hanyu 181#, Shapingba District, Chongqing 400030, China. Tel: +86-023-65311341; E-mail: sunhao782@163.com

References

[1] Bray F, Ferlay J, Soerjomataram I, Siegel RL, Torre LA and Jemal A. Global cancer statistics 2018: GLOBOCAN estimates of incidence and mortality worldwide for 36 cancers in 185 countries. CA Cancer J Clin 2018; 68: 394-424.

[2] Akakura K. Editorial comment to external beam radiotherapy and radical prostatectomy are associated with better survival in Asian prostate cancer patients. Int J Urol 2022; 29: 24-25.

[3] Liu Y, Zhou JW, Liu CD, Yang JK, Liao DY, Liang ZJ, Xie X, Zhou QZ, Xue KY, Guo WB, Xia M, Zhou JH, Bao JM, Yang C, Duan HF, Wang HY, Huang ZP, Zhao SC and Chen MK. Comprehen-

sive signature analysis of drug metabolism differences in the white, black and asian prostate cancer patients. Aging (Albany NY) 2021; 13: 16316-16340.
[4] Diermeier SD, Chang KC, Freier SM, Song J, El DO, Krasnitz A, Rigo F, Bennett CF and Spector DL. Mammary tumor-associated RNAs impact tumor cell proliferation, invasion, and migration. Cell Rep 2016; 17: 261-274.
[5] Zhang Y, Han P, Guo Q, Hao Y, Qi Y, Xin M, Zhang Y, Cui B and Wang P. Oncogenic landscape of somatic mutations perturbing pancancer lncRNA-ceRNA regulation. Front Cell Dev Biol 2021; 9: 658346.
[6] Wu X, Xiao Y, Zhou Y, Zhou Z and Yan W. LncRNA FOXP4-AS1 is activated by PAX5 and promotes the growth of prostate cancer by sequestering miR-3184-5p to upregulate FOXP4. Cell Death Dis 2019; 10: 472.
[7] Zhang G, He X, Ren C, Lin J and Wang Q. Long noncoding RNA PCA3 regulates prostate cancer through sponging miR-218-5p and modulating high mobility group box 1. J Cell Physiol 2019; 234: 13097-13109.
[8] Hagemann N, Ackermann N, Christmann J, Brier S, Yu F and Erdmann KS. The serologically defined colon cancer antigen-3 interacts with the protein tyrosine phosphatase PTPN13 and is involved in the regulation of cytokinesis. Oncogene 2013; 32: 4602-4613.
[9] Yu F, Sharma S, Skowronek A and Erdmann KS. The serologically defined colon cancer antigen-3 (SDCCAG3) is involved in the regulation of ciliogenesis. Sci Rep 2016; 6: 35399.
[10] Sunkel B, Wu D, Chen Z, Wang CM, Liu X, Ye Z, Horning AM, Liu J, Mahalingam D, Lopez-Nicora H, Lin CL, Goodfellow PJ, Clinton SK, Jin VX, Chen CL, Huang TH and Wang Q. Integrative analysis identifies targetable CREB1/FoxA1 transcriptional co-regulation as a predictor of prostate cancer recurrence. Nucleic Acids Res 2017; 45: 6993.
[11] Bruford EA, Antonescu CR, Carroll AJ, Chinnaiyan A, Cree IA, Cross N, Dalgleish R, Gale RP, Harrison CJ, Hastings RJ, Huret JL, Johansson B, Le Beau M, Mecucci C, Mertens F, Verhaak R and Mitelman F. HUGO Gene Nomenclature Committee (HGNC) recommendations for the designation of gene fusions. Leukemia 2021; 35: 3040-3043.
[12] Tomczak K, Czerwinska P and Wiznerowicz M. The Cancer Genome Atlas (TCGA): an immeasurable source of knowledge. Contemp Oncol (Pozn) 2015; 19: A68-A77.
[13] Paraskevopoulou MD, Georgakilas G, Kostoulas N, Reczko M, Maragkakis M, Dalamagas TM and Hatzigeorgiou AG. DIANA-LncBase: experimentally verified and computationally predicted microRNA targets on long non-coding RNAs. Nucleic Acids Res 2013; 41: D239-D245.
[14] Dweep H, Sticht C, Pandey P and Gretz N. MiRWalk--database: prediction of possible miRNA binding sites by "walking" the genes of three genomes. J Biomed Inform 2011; 44: 839-847.
[15] Mon-Lopez D and Tejero-Gonzalez CM. Validity and reliability of the TargetScan ISSF Pistol & Rifle application for measuring shooting performance. Scand J Med Sci Sports 2019; 29: 1707-1712.
[16] Zhu X, Jiang L, Yang H, Chen T, Wu X and Lv K. Analyzing the lncRNA, miRNA, and mRNA-associated ceRNA networks to reveal potential prognostic biomarkers for glioblastoma multiforme. Cancer Cell Int 2020; 20: 393.
[17] Yu Y, Gao F, He Q, Li G and Ding G. LncRNA UCA1 functions as a ceRNA to promote prostate cancer progression via sponging miR143. Mol Ther Nucleic Acids 2020; 19: 751-758.
[18] Kobayashi H and Tomari Y. RISC assembly: coordination between small RNAs and Argonaute proteins. Biochim Biophys Acta 2016; 1859: 71-81.
[19] Miao H, Wang L, Zhan H, Dai J, Chang Y, Wu F, Liu T, Liu Z, Gao C, Li L and Song X. A long noncoding RNA distributed in both nucleus and cytoplasm operates in the PYCARD-regulated apoptosis by coordinating the epigenetic and translational regulation. PLoS Genet 2019; 15: e1008144.
[20] Cai R, Sun Y, Qimuge N, Wang G, Wang Y, Chu G, Yu T, Yang G and Pang W. Adiponectin as lncRNA inhibits adipogenesis by transferring from nucleus to cytoplasm and attenuating Adiponectin mRNA translation. Biochim Biophys Acta Mol Cell Biol Lipids 2018; 1863: 420-432.
[21] Zhang K, Shi ZM, Chang YN, Hu ZM, Qi HX and Hong W. The ways of action of long non-coding RNAs in cytoplasm and nucleus. Gene 2014; 547: 1-9.
[22] Sharma S, Carmona A, Skowronek A, Yu F, Collins MO, Naik S, Murzeau CM, Tseng PL and Erdmann KS. Apoptotic signalling targets the post-endocytic sorting machinery of the death receptor Fas/CD95. Nat Commun 2019; 10: 3105.
[23] Mcmullin RP, Dobi A, Mutton LN, Orosz A, Maheshwari S, Shashikant CS and Bieberich CJ. A FOXA1-binding enhancer regulates Hoxb13 expression in the prostate gland. Proc Natl Acad Sci U S A 2010; 107: 98-103.
[24] Palit SA, Vis D, Stelloo S, Lieftink C, Prekovic S, Bekers E, Hofland I, Sustic T, Wolters L, Beijersbergen R, Bergman AM, Gyorffy B, Wessels LF, Zwart W and van der Heijden MS. TLE3 loss confers AR inhibitor resistance by facilitating

GR-mediated human prostate cancer cell growth. Elife 2019; 8: e47430.
[25] Foley C and Mitsiades N. Moving beyond the androgen receptor (AR): targeting AR-interacting proteins to treat prostate cancer. Horm Cancer 2016; 7: 84-103.
[26] Goel S, Bhatia V, Kundu S, Biswas T, Carskadon S, Gupta N, Asim M, Morrissey C, Palanisamy N and Ateeq B. Transcriptional network involving ERG and AR orchestrates distal-less homeobox-1 mediated prostate cancer progression. Nat Commun 2021; 12: 5325.

Table S1. The primers and sequencing results of RACE of lncHUPC1

A: 5-RACE Primer name and sequence	
Primer	sequence (5' to 3')
rAC004447.2-R1	GCTCTCTGAACAGTTGCCATACTTGAGT
rAC004447.2-R2	GCATCTTGAGAGACTTAATGAAATTTTAGC
B: 5-RACE Primer name and sequence	
Primer	sequence (5' to 3')
rAC004447.2-F1	GCTAACAGAGCACTTCTGGAGAGCAATGG
rAC004447.2-F2	GAGGAGCTGGTTCCTCAGCACTCACA
C: The gene sequence of lncHUPC1 (lncRNA AC004447.2)	

TGCATTTCCTCTACATTTATTGCAACGGCTAAATGATTAACAACATTCACAACTTCTTAGATCTTAAAAAACAGAAA-
CAAAAGAAAACTTCCATTTTGTAACATCACAAATGTCTTCTAGGCTTTATCAAGGACCAAAAACACTACAATTCTCTAAGTGATTTC-
CAGTGATGGAAACAAGCCAGAGACAGTAAAGCACCCAGAGTGGCGAGAGAGCACTTCCAGATGCCTGTTGTCCTCTCGGGGGT-
GACCCTGGAACTAGAACGACAGAAAAGACACTGTGACTTTGACACGGCTGTGCCACCACACATCACGCGCGACACGAG-
GATCCTGCAGAGCGGCCTCTGCAGAGAGCAAGGACAGCCTCGGTTAAGAGGGAGGGGCTGGGGGCACGGAGGGCCAGTG-
GCATCTCCTCTATCCCGGCTGGCCGGCAGCTGGCAGCACGCACCATGCTCTGCTGGCTCCCGACACCTTCACTGCCCCAGC-
GCTGAATCCACAGGAGAGGTGTCCTCTGAGAGTGTAGGGGGCTTTCTAGGTTCAAGGAGATGTGCCCTTTGACCCCTGC-
CAAGGACTCACAGAACCATCTCAGCTCAAACTTGGAGGAGCGGCAGGAGGTGGGGGGCGGTCAGTGGCCACACGCCA-
CAGATTCCTAAAGCATTTAACTTTTTAATAAAATGAAGTGGAGAAAGTCAAGAATGAACATGCTAGGACAAAGCACATGGAATG-
GTCAGGGCGATGCTGGAGAGAGTGCGCTTGATCCACGCTGCAGGTGTGTGCGCCTCGCTCGGGTCAATGGGCTGAGCCCC-
GCTTGGAGCTCCATCCATTCACCTGACCCATGGCCAACATGGAAGCTGTCGGAGGGGTCAGGAAAGGAGAAGGAGAAAGGA-
GATGATGAACCCCCCGCACCTGTGACTCCCCAAAACCAGCTCCACTCCAGGCCCCCACAGGCTGGTTCGTTCGAGGGTTGGGT-
TATAAACCCAAACTCCATCCTCCATGCTGGCACCTCTACTGCCATAAAGATCTGCCAGTTGCCAAAGCTACAGAAGC-
CACTGGAAGCAAGCAGAGCCCCTGGGGGTGGTGGCACTGCAAGGTGACAGGGACCAGGCAGACAAGGAGCTGGGACCA-
CAGCCTAGGAAGTCTGTGGCTTAAAGAAAGCCAGGATTTCCTTTTTTTTTTTTTGAGACAGAGTCTCGCTCTGTTGCCAGGCTG-
GAGTGCGGTGGCACAATCTCGGCTCACTGCAACCTCCGCCTCCCGGGTTCAAGTGATTCTCCTGCCTCAGCCTCCTGAG-
TAGCTGGGACTACAAGCGCCCGCCACCACGCCCAGCTAATTTTTTGCATTTTTAGTAGAGACAGGGTTTCACCATGTTGGCCAG-
GATGGTCTCGATCTCTTGACCTCGTGATCCACCTGCCTCGGCCTCCCAAAGTGCTGGAATTATAGGCGTGAGTCACCGTGC-
CGGCCTTTTTTTTTTTTTTTTTGGAGATGGAGTCTTGCTCTGTCGCCCAGGCTGGAGTGGAGTGGCATGATCTCAGCTCACTG-
CAACCTCTGCCTCCCCGGTTCAAGTGATTCTCCTGCCTCAGCCTCCTGAGTAGCTGGGATTACAGGTGCCCGCTACCACGCCTG-
GCTAATTTTTTTGTATTTTTAGTAGAGACGGGGTTACACCATGTTGGCCAGGCTGGTCTCAAACTCCTGACCTCAGGTGATCCATC-
CGCCTCAACCTCCTAAAGTGCTGGGATTACAGGCTTGAGCCACTGTGCCTGGCCCAAAGCCAGGATTTCTTTACAGCCAATA-
CAAGTGGCATTTCCCGCTCAGTTCTGTGGCTGATGCCCTAGCCACTGCTGTGTCCCCTAATCCTGGGGTGTCAGAGGGATCCTA-
AGTTTTCCAGATTTTTGCCCATACTTAAAACTTCAACGATCCTGCTTCACAAGGAAGGATGAGTGGAGAATTGAGTGGAGTTACAC-
GCAGCAGAGTGCTGGGGAATCTGGAGAGCGGGGGCGATCACATGCCTGGAAATAGAGCAGCTGCAGAGCCCACCCCAGGAG-
GAGCCTGCCTCTCCTTACAAAGGCTGTAATAAGACAGCACTTGACGATGCCATACGTGCGAAAAGTGCAGAGTCTCAGAGGGTT-
TACAACCCCCATCCCTTTGTAACTGTAGTTTGCTTACACTGTGGATTCTAAAGAGACATGTAAATCTGGGGCCGATTTCATCTGTT-
TAATGATTACTCCCCACCCGATAGAGCTATTCTATACTGTTGCTAAAATTTCATTAAGTCTCTCAAGATGCATTGATGAGATGAGACAC-
CATGAATAACACATTCATCAACTCAAGTATGGCAACTGTTCAGAGAGCTTCAGAGCTTTGGTACCCGAGTGCAGACTTGGTAATTAC-
CGGGAATTTGTCTCCCCCGTATAAATTCTGGCGAACAACGAGAAAACACCATCTGTGATCGTTTCCACATCACGTTTGCTAACAGAG-
CACTTCTGGAGAGCAATGGCCAGTCCAACTGGAAAATCAGCCAGAGGAGCTGGTTCCTCAGCACTCACAGGCTGAGGTGC-
CTTTCGGGGGCAGCGCCACCTTCTGAAGGGGAACCAAGACAGATTTGGAGGGGACTTGCTGCTAAAAGCATGTGAACAGAGAG-
GAGAGGCAAAAGCACATTGAAAATGGTGCATGTTTTTTTCTTTGAGAGAAAGAAAAGCCAGCGAAACCTCCGCCCCAGAGACT-
GCAGAGACGTTTGTTTTCATGTACACACCAAACCGTACTTGGGCACTGGCTCCAGGCCGATCCAGGGCAGGGATGATGTTTTA-
AGGGCAATTGCTGCTTCAAGGCTTATCTTTCACATCAGTGGTTTTGATCTATTCAGGAAGAGAACGATTTTGTTCAAAACTGAGGTG-
GAAATTAGGTGAGGGGGCAACTAAAAAAAAAAAAAAA